CD4 downregulation precedes Env expression and protects HIV-1-infected cells from ADCC mediated by non-neutralizing antibodies

Jonathan Richard [1,2,#], Gérémy Sannier [1,2,#], Li Zhu[3,#], Jérémie Prévost [1,2], Lorie Marchitto [1,2], Mehdi Benlarbi [1,2], Guillaume Beaudoin-Bussières [1,2], Yaping Sun [3], Kim Hongil [3], Debashree Chatterjee[1], Halima Medjahed[1], Catherine Bourassa[1] Gloria-Gabrielle Delgado[1], Mathieu Dubé[1], Frank Kirchhoff[4], Beatrice H. Hahn[5,6], Priti Kumar[3,*], Daniel E. Kaufmann[7,8,9,*], Andrés Finzi[1,2,*].

[1]Centre de Recherche du CHUM, Montreal, Quebec, Canada
[2]Département de Microbiologie, Infectiologie et Immunologie, Université de Montréal, Montreal, Québec, Canada
[3]Department of Internal Medicine, Section of Infectious Diseases, Yale University School of Medicine, New Haven, Connecticut, USA
[4]Institute of Molecular Virology, Ulm University Medical Center , Ulm, Germany
[5]Department of Medicine, Perelman School of Medicine, University of Pennsylvania , Philadelphia, Pennsylvania, USA.
[6]Department of Microbiology, Perelman School of Medicine, University of Pennsylvania , Philadelphia, Pennsylvania, USA.
[7]Department of Medicine, Université de Montréal, Montreal, Quebec, Canada
[8]Center for HIV/AIDS Vaccine Immunology and Immunogen Discovery, The Scripps Research Institute, La Jolla, California, USA
[9]Division of Infectious Diseases, Department of Medicine, Lausanne University Hospital and University of Lausanne, 1011 Lausanne, Switzerland
[#]co-first authors

*Correspondence:
to **Andrés Finzi**, Centre de recherche du CHUM (CRCHUM), 900 St-Denis street, Tour Viger, R09.420, Montréal, Québec, H2X 0A9, Canada ; Phone: 514-890-8000 ext: 35264; email: andres.finzi@umontreal.ca. Or to **Daniel E. Kaufmann**, Lausanne University Hospital and University of Lausanne, Rue du Bugnon 46, 1011 Lausanne, Switzerland; Phone: +41 21 314 10 10; email: daniel.kaufmann@chuv.ch. Or to **Priti Kumar**, Department of Internal Medicine, Section of Infectious Diseases, Yale University School of Medicine, 25 York St, New Haven, CT 06511; Phone: 203.737.3580; email: priti.kumar@yale.edu

Authorship note: JR, GS and LZ contributed equally to this work and PK, DEK and AF contributed equally as co-senior authors. AF is the lead contact

Conflict of interest: The authors have declared that no conflict of interest exists
Word count (all text): 10683/12000

SUMMARY (192/200 words)

HIV-1 envelope glycoprotein (Env) conformation substantially impacts antibody-dependent cellular cytotoxicity (ADCC). Envs from primary HIV-1 isolates adopt a prefusion “closed” conformation, which is targeted by broadly-neutralizing antibodies (bnAbs). CD4 binding drives Env into more “open” conformations, which are recognized by non-neutralizing Abs (nnAbs). To better understand Env-Ab and Env-CD4 interaction in CD4+ T cells infected with HIV-1, we simultaneously measured antibody binding and HIV-1 mRNA expression using multiparametric flow cytometry and RNA-flow fluorescent *in situ* hybridization (FISH) techniques. We observed that *env* mRNA is almost exclusively expressed by HIV-1 productively-infected cells that already downmodulated CD4. This suggest that CD4 downmodulation precedes *env* mRNA expression. Consequently, productively-infected cells express “closed” Envs on their surface, which renders them resistant to nnAbs. Cells recognized by nnAbs were all *env* mRNA negative, indicating Ab binding through shed gp120 or virions attached to their surface. Consistent with these findings, treatment of HIV-1 infected humanized mice with the ADCC mediating nnAb A32 failed to lower viral replication or reduce the size of the viral reservoir. These findings confirm the resistance of productively-infected CD4+ T cells to nnAbs-mediated ADCC and question the rationale of immunotherapy approaches using this strategy.

60 **INTRODUCTION**

61 Highly active antiretroviral therapy (ART) efficiently suppresses HIV-1 replication and
62 significantly increase the life expectancy of people living with HIV-1 (PLWH) (1, 2).
63 However, it has become evident that even lifelong ART cannot eradicate the virus. Viral
64 reactivation and rebound can occur upon treatment interruption due to the presence of a
65 latent reservoir, persisting mainly in long-lived memory CD4+ T cells (3-6). New
66 approaches aimed at eradicating or functionally curing HIV-1 infection by targeting and
67 eliminating productively or latently-infected cells are needed. Monoclonal antibodies
68 (mAbs) are attractive therapeutics for HIV cure strategies, since they target virus specific
69 antigens and have the potential to harness host immune responses such as antibody-
70 dependent cellular cytotoxicity (ADCC). The HIV-1 envelope glycoprotein (Env) is the only
71 viral antigen that is present on the surface of HIV-1-infected cells, thus representing the
72 main target for immunotherapy-based strategies (7). In recent year, several clinical trials
73 explored broadly-neutralizing antibodies (bnAbs) as therapeutic agents to reduce the HIV-
74 1 reservoir via Fc-mediated effector functions (8). Monotherapy or combination of bnAbs
75 targeting multiple regions of the Env trimer including the V3 glycan supersite (10-1074,
76 PGT121), the V2 apex (PGDM 1400, CAP256-VRC26), or the CD4 binding site (CD4bs)
77 (3BNC117, N6, VRC01, VRC07-523) are currently under investigation. Administration of
78 bnAbs to humans has been found to be safe and effective in lowering viremia and
79 maintaining viral suppression for varying periods of time after treatment interruption (9-
80 15). However, recent data suggest that bnAbs may not be as broad and/or effective as
81 predicted, in part because of circulating viruses with pre-existing resistance to the
82 administered bnAbs (8). So-called “non-neutralizing” Abs (nnAbs) have been evaluated
83 as a potential alternative, because they target highly conserved Env epitopes that are
84 usually occluded in the closed trimer, including the coreceptor-binding site (CoRBS) (16-
85 18), the inner domain of gp120 (19-21) or the gp41 immunodominant domain (gp41ID)

86 (22). These nnAbs are naturally elicited during HIV-1 infection and can mediate potent Fc
87 effector functions (22-28).
88
89 HIV-1 Env is a conformationally flexible molecule that transitions from an
90 unliganded “closed” State 1 conformation to an “open” CD4-bound State 3 conformation
91 (29-31) upon CD4 interaction. Envs from most primary HIV-1 isolates adopt a “closed”
92 conformation that is efficiently targeted by bnAbs, but is resistant to nnAbs (29, 32-36),
93 which target epitopes that are occluded within the unliganded “closed” trimer. Env
94 interaction with CD4 or small CD4-mimetic compounds are known to induce more “open”
95 conformations, thus sensitizing infected cells to ADCC mediated by CD4-induced (CD4i)
96 nnAbs (23, 24, 26, 27, 33, 34, 36-42). To avoid exposing these nnAb epitopes, the Env
97 trimer is stabilized by multiple intermolecular interactions, including between the V1, V2
98 and V3 variable loops as well as the gp120 β20–β21 element, which maintain a “closed”
99 conformation (31, 43, 44). In addition, HIV-1 expresses the accessory proteins Nef and
100 Vpu, which indirectly modulate Env conformation by downregulating CD4 from the surface
101 of infected cells, thus preventing a premature Env-CD4 interaction that would otherwise
102 result in the exposure of CD4i Env epitopes (23, 26). Vpu-mediated counteraction of the
103 restriction factor BST-2 (also named “tetherin”), known to tether viral particles at the
104 surface of infected cells, also reduces cell-surface levels of Env (23, 26, 45, 46).
105
106 Despite advances in understanding Env-Ab and Env-CD4 interactions, the
107 capacity of nnAbs to target and eliminate productively-infected cells by ADCC remain
108 controversial. Several studies reported that cells infected with primary viruses expressing
109 functional Vpu and Nef proteins are resistant to ADCC mediated by CD4i nnAbs, because
110 they maintain surface expressed Env in a “closed” conformation (23, 24, 27, 32-42, 47,
111 48). Other studies report that CD4i nnAbs can mediate ADCC responses, but they have

112 used infectious molecular clones (IMCs) that are defective for Nef expression (49-60).
113 These IMCs contain reporter genes (e.g., the Renilla luciferase [LucR] gene) upstream of
114 the *nef* gene, which significantly reduces Nef expression and thus CD4 downregulation
115 from the surface of infected CD4+ target cells. The resulting premature Env-CD4
116 interaction promotes the artificial exposure of otherwise occluded CD4i epitopes (39, 61,
117 62).
118
119 Here, we used multiparametric flow cytometry and RNA-flow fluorescent *in situ*
120 hybridization (FISH) techniques to characterize cell populations targeted by bNAbs and
121 nnAbs in the context of primary CD4+ T cell infection. We show that *env* mRNA is
122 specifically detected among cells that already downmodulated cell-surface CD4, which
123 renders these cells refractory to recognition by nnAbs. Although some CD4+ cells are
124 bound by nnAbs, they are all negative for *env* mRNA, indicating that they are not
125 productively-infected and nnAbs binding is mediated through the recognition of shed
126 gp120 and/or viral particles coated at their cell surface. The same results were obtained
127 with *ex vivo*-expanded CD4+ T cells isolated from PLWH. Finally, the ADCC mediating
128 nnAb A32 failed to reduce HIV-1 replication and the size of the viral reservoir in a
129 humanized mouse model (hu-mice) that supports Fc-effector functions. These findings
130 raise questions about curative immunotherapy-based strategies that rely solely on nnAbs,
131 specifically those targeting CD4i epitopes.

132 **RESULTS**

133

134 **Expression of CD4, p24 and Nef defines recognition of HIV-1 infected CD4+ T cells**
135 **by nnAbs and bnAbs**

136 To characterize cell populations targeted by nnAbs and bnAbs in HIV-1-infected
137 primary CD4+ T cells, we used multiparametric flow cytometry to simultaneously probe
138 CD4 and viral proteins expression. Activated primary CD4+ T cells were mock-infected or
139 infected with the transmitted-founder virus CH077 (CH077TF). Two days post-infection,
140 cells were stained with a panel of nnAbs and bnAbs, followed by appropriate secondary
141 Abs. Cells were then stained for cell-surface CD4 prior to staining for intracellular HIV-1
142 p24. Given that the *nef* gene is abundantly expressed during the early phase of the HIV-
143 1 replication cycle (63, 64), we also evaluated the expression of this accessory protein by
144 intracellular staining as previously described (61). The different cell populations were
145 gated based on cell-surface CD4 and intracellular p24 detection as shown in Figure 1A.
146 As expected, uninfected $CD4^{+}p24^{-}$ cells were not recognized by bnAbs of various
147 specificities (PGT126, PG9, 3BNC117, PGT151 and 2G12) (Figure 1B-D). Interestingly,
148 this population was efficiently recognized by CD4i nnAbs targeting the coreceptor-binding
149 site (17b) or the gp120 inner domain (A32, C11) as well as a pool of purified
150 immunoglobulins from PLWH (HIV-IG). However, the $CD4^{+}p24^{-}$ cells were not recognized
151 by the CD4i gp41-specific nnAbs F240. The absence of binding by bnAbs and F240
152 suggested that these cells were likely coated with shed gp120 rather than presenting CD4-
153 bound cell-surface Env trimer. This is in line with previous work showing that uninfected
154 CD4+ T cells expose CD4i epitopes on their cell surface after interacting with gp120 shed
155 from productively-infected cells within the same culture (33, 65, 66). Indeed, introduction
156 of a CD4bs (D368R) mutation into CH077TF that prevents Env-CD4 interaction (17, 23,

157 67), abrogated the recognition of the $CD4^{+}p24^{-}$ population by all gp120-specific nnAbs
158 tested (Figure S1A-B).
159
160 In addition to productively infected CD4+ T cells, which efficiently downregulated
161 CD4 ($CD4^{low}p24^{high}$), we identified a subset of $CD4^{+}p24^{low}$ cells , as previously reported
162 (51, 58, 68-72). This $CD4^{+}p24^{low}$ subset was efficiently recognized both by the gp120-
163 specific nnAbs and HIV-IG, but was resistant to bnAbs binding. This population was also
164 recognized by the gp41-specific F240 nnAb, suggesting the presence of trimeric Env
165 bound to CD4. However, recognition of the $CD4^{+}p24^{low}$ cells by CD4i nnAbs was
166 substantially reduced upon the introduction of the D368R mutation (Figure S1A-B). This
167 mutation also specifically reduced the proportion of $CD4^{+}p24^{low}$ cells (Figure S1C). These
168 findings, along with the observation that these cells do not express Nef (Figure 2) suggest
169 that $CD4^{+}p24^{low}$ cells are not productively infected, but contain CD4-Env complexes on
170 their surface resulting from the binding of shed gp120 and/or viral particles.
171
172 As expected, cells that expressed high level of p24 ($CD4^{low}p24^{high}$) were poorly
173 recognized by nnAbs. We reasoned that this was because they efficiently downregulated
174 cell-surface CD4, which precludes premature Env triggering, and thus prevents the
175 exposure of normally occluded epitopes (23, 26, 33). $CD4^{low}p24^{high}$ cells also expressed
176 Nef (Figure 2) and were efficiently recognized by bnAbs, known to preferentially recognize
177 Env in its “closed” conformation (Figure 1B-D). However, when we used a *nef*-defective
178 virus these cells were efficiently recognized by nnAbs (Figure 1E-H), in agreement with
179 previous observations (26, 33, 37, 39, 61, 73, 74).
180
181 To test whether our findings extend to IMCs widely used in the ADCC field (28, 35,
182 53, 55, 68, 72, 75-77), we infected primary CD4+ T cells with with viruses produced from

183 a pNL4.3 backbone expressing different Envs, including BaL and NL4.3. As shown in
184 Figure S2A-B, the patterns of bnAbs and nnAbs binding were very similar to those
185 observed for CH077TF. The $CD4^{+}p24^{-}$ and $CD4^{+}p24^{low}$ cell populations were preferentially
186 recognized by the nnAbs, while the $CD4^{low}p24^{high}$ cells were efficiently targeted by the
187 bnAbs. Interestingly, despite similar levels of productive infection ($CD4^{low}p24^{high}$, Figure
188 S2C), an enrichement of the $CD4^{+}p24^{low}$ population was detected in the context of
189 infection with the NL4.3 and BaL Envs as compared to Envs from primary viruses
190 (CH058TF, CH040TF, SF162 and YU2) (Figure S2D). The reasons for this are unclear
191 but may be due to greater gp120 shedding of the tier 1 NL4.3 and BaL Envs.
192
193 Taken together, our results indicate that cells recognized by nnAbs express high
194 levels of CD4, are either $p24^{low}$ or $p24^{-}$, and are negative for Nef expression. In contrast,
195 bnAbs recognize cells that efficiently downregulate CD4 and express high level of p24 and
196 Nef proteins.
197
198 **e*nv* mRNA is predominantly detected in cells that already downregulated CD4**
199 To better understand the underlying mechanisms behind the differential recognition
200 of infected cells by bNAbs versus nnAbs, we used a previously described RNA-flow
201 cytometric fluorescence *in situ* hybridization (RNA Flow-FISH) method (78-80). This
202 method identifies productively-infected cells by detecting cellular HIV-1 mRNA by using *in*
203 *situ* RNA hybridization and intracellular Ab staining for the HIV-1 p24 protein. In the context
204 of these experiments, *env* and *nef* mRNA probes were used to identify productively-
205 infected CD4+ T cells. Briefly, primary CD4 T cells were mock-infected or infected with
206 the CH077TF IMC. Two days post-infection, cells were stained for surface CD4 before
207 fixation and permeabilization to allow detection of the HIV-1 p24 antigen and HIV-1
208 mRNAs. Cell populations were first defined based on their cell-surface CD4 and

209 intracellular p24 co-expression, as presented in Figure 3A. Productively-infected cells
210 were identified as *nef* mRNA+/*env* mRNA+.The vast majority of cells with detectable cell-
211 surface CD4 ($CD4^{+}p24^{-}$ or $CD4^{+}p24^{low}$) were negative for HIV-1 mRNA (Figure 3B-C),
212 while cells that efficiently downmodulated CD4 ($CD4^{low}p24^{low}$ and $CD4^{low}p24^{high}$) were
213 enriched for *nef* and *env* mRNA transcripts (Figure 3B-C; Figure S3). When gating on
214 productively-infected cells based on *nef* and *env* mRNA detection, we confirmed that the
215 $CD4^{low}p24^{high}$ cells represent the major source of productively-infected cells (Figure 3D-
216 E). These results show that *env* mRNA is predominantly expressed by HIV-1-infected cells
217 that already downregulated CD4 ($CD4^{low}p24^{low}$ and $CD4^{low}p24^{high}$) (Figure S3). This
218 analysis also captured stages of infection ($CD4^{low}p24^{low}$) where CD4 is already
219 downmodulated while *env* mRNA expression intensifies, suggesting that CD4
220 downmodulation precedes *env* mRNA expression.
221
222 **Cells targeted by A32 are negative for HIV-1 mRNA**
223 We next combined flow cytometry and RNA flow-FISH methods to compare the
224 capacity of nnAbs and bnAbs to bind productively-infected cells. Mock-infected or
225 CH077TF-infected primary CD4 T cells were first stained with the nnAb A32 or the bNAb
226 PGT126. Cells where then stained for cell-surface CD4 detection, intracellular p24 and
227 HIV-1 mRNAs. Productively-infected cells were identified based on the simultaneous
228 detection of *nef* and *env* mRNA transcripts (Figure 4A). As shown in Figure 4B-C,
229 productively-infected cells (*env*/*nef* mRNA+ cells) were recognized by PGT126, but not by
230 A32. In contrast, *env*/*nef* mRNA- cells were targeted by A32, but not by PGT126. Similar
231 results were obtained when cells were classified by Ab recognition (Figure 4D-F; Figure
232 S4), with the majority of PGT126+ cells co-expressing HIV-1 mRNA. In contrast, cells
233 recognized by A32 were negative for *env* and *nef* mRNA (Figure 4E-F; Figure S4). These

234 results indicate that cells targeted by A32 do not express *env* mRNA (Figure S4), are not
235 productively infected and thus are likely coated with gp120 and/or viral particles.
236
237 ***Ex vivo* expanded CD4+ T cells isolated from PLWH are resistant to ADCC**
238 **responses mediated by nnAbs**
239 Our results indicated that productively infected cells are principally $CD4^{low}p24^{high}$,
240 express *nef* and *env* mRNA and are not recognized by nnAbs. To confirm these findings
241 with primary clinical samples, we expanded CD4+ T cells from PLWH. Briefly, CD4+ T
242 cells were isolated from 6 chronically-infected individuals and activated *ex vivo* using PHA-
243 L/IL-2 (24, 38, 40). CD4+ T cells from people without HIV were used as controls. Viral
244 replication was monitored over time by intracellular p24 staining (Figure 5A). Upon
245 expansion, CD4+ T cells were stained with a panel of bnAbs and nnAb, followed by the
246 appropriate secondary Abs. Cells were stained for cell-surface CD4 prior to the detection
247 of intracellular HIV-1 p24 and Nef proteins. Consistent with the results obtained with IMC
248 infections (Figure 2), productively-infected $CD4^{low}p24^{high}$ cells were the only ones which
249 were also positive for the Nef protein (Figure S5). These cells were efficiently recognized
250 by bnAbs and largely resistant to nnAbs binding (Figure 5C,D, E). In contrast, nnAbs
251 mainly recognized CD4+ cells that were either $p24^{-}$ or $p24^{low}$ as well as negative for Nef
252 expression (Figure 5C, D, E; Figure S5). To evaluate the susceptibility of productively-
253 infected cells to ADCC responses mediated by bnAbs and nnAbs, expanded
254 endogenously-infected cells were used as target cells and autologous peripheral blood
255 mononuclear cells (PBMCs) as effectors using a FACS-based ADCC assay (Figure 6).
256 Consistent with antibody binding, productively-infected $CD4^{low}p24^{high}$ cells were resistant
257 to ADCC mediated by nnAbs, but sensitive to those mediated by bnAbs.
258
259

260 **A32 does not affect HIV-1 replication or the size of HIV-1 reservoir *in vivo*.**

261 Our results indicate that nnAbs, such as A32, target nonproductively-infected
262 CD4+ T cells. It has been suggested that these cells could be in a very early stage of
263 infection, during viral entry, before viral gene expression (81). Specifically, it has
264 previously been shown that non-neutralizing Env epitopes, such as that targeted by A32,
265 become transiently exposed during viral entry and could therefore represent a suitable
266 target for ADCC at this stage (81). We hypothesized that if this was the case, then this cell
267 population should be eliminated by A32 and therefore decrease HIV-1 replication *in vivo*.
268 To evaluate this possibility, we tested whether A32 affected viral replication in humanized
269 mice (hu-mice). Briefly, NOD.Cg-*Prkdc*^{scid} IL2rg$^{-/-}$ Tg(Hu-IL15) (NSG-15) hu-mice
270 engrafted with human peripheral blood lymphocytes (hu-PBL) were infected with the
271 primary isolate HIV-1_{JRCSF} (Figure 7A). This hu-mice model was previously shown to
272 support HIV-1 replication and antibody Fc-effector function *in vivo* (24, 82). Infected hu-
273 mice received nnAb A32 administered subcutaneously (S.C.) at day 6 and 9 post-infection
274 (Figure 7A). As controls, infected mice were also treated with the bnAbs 3BNC117 or its
275 Fc gamma receptor (FcγR) null binding variant (GRLR) (83). Hu-mice were monitored for
276 plasma viral loads (PVLs) and peripheral CD4+ T cells overtime (Figure 7B-C). In the
277 absence of antibody treatment, mice became viremic, reaching an average PVL of $2.2x10^7$
278 copies/mL at day 11. As previously reported (41, 82), viral replication was associated with
279 a loss of peripheral CD4+ T cells. Treatment with 3BNC117 WT significantly reduced viral
280 replication and partially restored CD4+ T cell levels in peripheral blood and several tissues,
281 while A32 failed to do so (Figure 7B,C,D). Interestingly, A32 treatment further reduced
282 CD4+ T cell levels in tissues relative to mock-treated mice (Figure 7D), consistent with its
283 capacity to recognize and eliminate uninfected bystander cells coated with soluble gp120
284 via ADCC (33, 65, 66). This reduction in CD4 T cells count was particularly significant
285 when CD4+ T cell levels where considered across all tissues in mice treated with A32

286 nnAb alone (Figure S6). Finally, treatment with 3BNC117 WT led to a significant reduction
287 of the HIV-1 reservoir in multiple tissues, a phenotype not observed with A32 and not fully
288 achieved by its FcγR null binding variant (3BNC117 GRLR, Figure 7E). These results are
289 in line with previous work demonstrating that bnAbs require Fc effector functions for *in*
290 *vivo* activity (83). These results indicate that A32 does not reduce HIV-1 replication or the
291 size of the reservoir in hu-mice.
292
293
294 **DISCUSSION**
295
296 ADCC represents an effective immune response involved in the clearance of
297 virally-infected cells. This adaptive immune response relies on the capacity of Abs to act
298 as a bridge between infected cells and effector cells. While the Abs recognize infected
299 cells through binding of surface Env via their Fab domain, their Fc domain allows the
300 recruitment and the stimulation of FcγR bearing effector cells, leading to the killing of
301 infected cells. ADCC-mediating Abs therefore represent attractive therapeutics for HIV
302 cure strategies. However, the ability of Abs to recognize productively-infected cells and to
303 mediate ADCC responses depends on Env conformation (73). While bnAbs target
304 epitopes on the prefusion "closed" Env trimer, nnAbs recognize conserved epitopes that
305 are normally occluded but are exposed when Env interacts with CD4 and adopt an "open"
306 conformation (29, 32-36). Here, we provide evidence that *env* mRNA expression is mainly
307 restricted to cells that already downmodulated cell-surface CD4 (Figures 3 and S3). This
308 prevents CD4i Env epitopes exposure on productively-infected cells, thus contributing to
309 their resistance to CD4i nnAbs.
310

311 Non-neutralizing Abs, such as those targeting the CoRBS and the inner domain of
312 gp120 are elicited during natural infection due to exposure to “viral debris” acting as
313 immunodominant decoy (23, 25, 28, 34, 84, 85). It is therefore not surprising that HIV-1
314 has evolved mechanisms to prevent surface Env-CD4 interaction to avoid Env recognition
315 by these nnAbs which have potent Fc-effector functions. HIV-1 utilizes Nef, Vpu and Env
316 to downmodulate CD4 from the surface of infected cells (86). Nef is expressed at high
317 levels early during infection from a multi-spliced transcript (63, 64) and downregulates
318 CD4 by enhancing its internalization and lysosome degradation (87-91). Vpu and Env are
319 expressed from a Rev-depended single spliced bicistronic mRNA later during the viral life
320 cycle (92). Both Vpu and Env interfere with the transport of newly synthesized CD4 to the
321 cell surface (93-95). Using RNA-Flow FISH methods, we show that *env* mRNA is almost
322 exclusively detected in cells positive for *nef* mRNA that efficiently downregulated CD4.
323 The majority of cells expressing HIV-1 mRNA substantially downregulated surface CD4
324 and express high levels of p24 and Nef proteins ($CD4^{low}p24^{high}$ cells). We also captured
325 stage of infection ($CD4^{low}p24^{low}$) where CD4 is already downmodulated while *env* mRNA
326 and p24 are not fully expressed. This suggest that Nef-mediated CD4 downmodulation
327 precedes Env expression (Figure 3 and S3). Accordingly, productively-infected cells failed
328 to expose CD4i epitopes, explaining their resistance to ADCC mediated by nnAbs, while
329 showing susceptibility to ADCC mediated by bNabs (Figure 1, 4, 5 and 6).
330
331 Our findings are consistent with a growing number of studies demonstrating the
332 importance of bnAbs in mediating ADCC against cells productively infected with primary
333 HIV-1 isolates (32, 33, 35). nnAbs recognize productively-infected cells only when CD4 is
334 not properly downregulated, as is the case in infections with Nef defective virus (Figure
335 1). This is also the case when *nef*-deficient IMCs are used for ADCC detection (28, 49-60,
336 69, 71, 76). Most of these IMCs express the Renilla luciferase (LucR) reporter gene

337 upstream of the *nef* sequence and use a T2A ribosome-skipping peptide to promote Nef
338 expression (62). Despite documented evidence of reduced Nef expression (39, 61, 62),
339 these IMCs continue to be used in the ADCC field (51, 52, 54, 55, 57, 58, 96). While some
340 studies have suggested that Vpu can compensate for the absence of Nef (51, 52), our
341 findings refute this. Given its early expression and ability to target cell surface expressed
342 CD4 molecules, Nef plays the most prominent role in CD4 downmodulation (61, 86, 97).
343 In absence of Nef expression, we find that Vpu is not sufficient to downregulate cell-
344 surface CD4, leading to CD4i epitope exposure and efficient nnAbs binding (Figure 1).
345 Other studies reporting Fc-effector functions of nnAbs employed assays unable to
346 differentiate the ADCC responses directed against HIV-1-infected cells versus uninfected
347 bystander cells (45, 49, 76, 98, 99). The presence of uninfected bystander cells coated
348 with gp120 shed from productively-infected cells impacts ADCC measurement by
349 introducing a significant bias toward CD4i nnAbs (33), which is also the case when ADCC
350 assays rely solely on target cells coated with gp120 or inactivated virions (33, 50, 60, 71,
351 72, 100, 101). Utilization of such assays, as well as *nef*-defective IMCs, contribute to the
352 propagation of a misleading concept that nnAbs can effectively mediate ADCC against
353 HIV-1-infected cells. nnAbs such as A32 not only fail to eliminate HIV-1-infected cells, but
354 also have potentially detrimental effects by accelerating the elimination of uninfected
355 bystander cells (33, 66), as shown in tissues of HIV-1-infected humanized mice (Figure 7;
356 Figure S6). In this context, the absence of an antiviral effect of A32 in hu-mice is not
357 surprising. Studies in non-human primate showed that elicitation of A32-like Abs by gp120
358 immunization or passive administration of A32 failed to confer protection against simian-
359 human immunodeficiency virus challenges (77, 102). Similarly, a combination of anti-
360 CoRBS and anti-cluster A (A32) nnAbs proved ineffective in delaying viral rebound after
361 ART interruption in humanized mouse model supporting Fc effector functions (41).
362

363 The inability of A32 to recognize productively-infected cells, to influence viral
364 replication and reduce the size of reservoir in hu-mice is a function of its epitope, which is
365 occluded in the unliganded trimer. To our knowledge, exposure of this epitope at the
366 surface of productively infected cells is possible in only two ways: either by membrane-
367 bound CD4 (26) or the combination of potent small CD4-mimetic compounds (CD4mc)
368 and anti-CoRBS Abs (27, 41). Of note, the cocktail of A32, 17b (CoRBS Ab) and CD4mc
369 was reported to significantly reduce the size of the reservoir in hu-mice (41).
370
371 In conclusion, we show that *env* mRNA is almost exclusively expressed by
372 productively-infected cells that downregulated cell-surface CD4. This suggests that CD4
373 downmodulation precedes Env expression, thus preventing exposure of vulnerable CD4-
374 induced Env epitopes and evading ADCC mediated by nnAbs. These results must be
375 taken into account when considering the use of nnAbs for preventative or cure strategies.
376

ACKNOWLEDGMENTS

The authors thank the CRCHUM BSL3 and Flow Cytometry Platforms for technical assistance, and Mario Legault from the FRQS AIDS and Infectious Diseases network for cohort coordination and clinical samples. We thank the following collaborators for kindly providing plasmids to produce antibodies: James Robinson (Tulane University) for A32 and C11, the NIH AIDS Reagent Program for F240, 2G12 and 17b, John Mascola (Vaccine Research Center, NIAID) for VRC03, the International AIDS Vaccine Initiative (IAVI) for PG9, PGT121, PGT126 and PGT151 and Michel Nussenzweig (Rockefeller University) for 3BNC117 and 10-1074.

This study was supported by grants from the National Institutes of Health to A.F. (R01 AI148379 and R01 AI150322, R01 AI129769, R01AI176531) and P.K. (R01AI145164). Support for this work was also provided by P01 GM56550/AI150471 to A.F., a Canadian Institutes of Health Research (CIHR) Team grant #422148 to D.E.K, P.K. and A.F., a CIHR foundation grant #352417 to A.F. and a Canada Foundation for Innovation (CFI) grant #41027 to D.E.K. and A.F. This work was partially supported by UM1AI144462 (CHAVD) (D.E.K), UM1AI164562 (ERASE) to A.F., and P.K., and UM1AI164559 (HOPE) to P.K., and by an American Foundation for AIDS Research (amfAR) Mathilde Krim Fellowship in Basic Biomedical Research (109720-63-RKRL) to J.R. A.F. was supported by a Canada Research Chair on Retroviral Entry #RCHS0235 950-232424. B.H.H. is supported by R01 AI162646, UM1AI144371 and UM1AI164570. J.P. was supported by a CIHR doctoral fellowship. M.B. was supported by a FRQS master's fellowship. G.B.B was supported by a FRQS and a CIHR doctoral fellowship. FK is supported by the German Research Foundation (DFG, CRC 1279) and an ERC Advanced grant (Traitor viruses). The funders had no role in study design, data collection and analysis, decision to publish, or preparation of the manuscript.

AUTHOR CONTRIBUTIONS

Conceptualization: J.R., G.S, L.Z, P.K., D.E.K and A.F.; **Methodology:** J.R, G.S, J.P., L.Z..,M.D., P.K., D.E.K. and A.F.; **Investigation:** J.R, G.S., L.Z., L.M., M.B., G.B.B., D.C., Y.S., H.K., J.P., H.M., C.B., and G.G.D.; **Resources:** J.R., G.S., J.P., L.Z., L.M., M.B., G.B.B., D.C., F.K., B.H.H., P.K., D.E.K. and A.F.; **Formal Analysis:** J.R., G.S. and L.Z.; **Visualization:** J.R., G.S and L.Z. **Supervision:** M.D., P.K., D.E.K. and A.F.; **Funding acquisition:** J.R. P.K., D.E.K. and A.F.; **Writing – original draft:** J.R., B.H.H., and A.F. **Writing – review & editing:** J.R., G.S., L.Z., J.P., L.M., M.B., G.B.B., D.C., F.K., B.H.H.,Y.S., H.K., H.M., C.B., G.G.D., M.D., P.K., D.E.K. and A.F.

416 **FIGURE LEGENDS**

417

418 **Figure 1. Recognition of HIV-1-infected primary CD4+ T cells by bnAbs and nnAbs.**
419 Primary CD4+ T cells, mock-infected or infected with the transmitted-founder virus CH077,
420 either wild-type (WT) or defective for Nef expression (*nef*-) were stained with a panel of
421 bnAbs and nnAbs, followed with appropriate secondary Abs. Cells were then stained for
422 cell-surface CD4 prior detection of intracellular HIV-1 p24. (A,E) Example of flow cytometry
423 gating strategy based on cell-surface CD4 and intracellular p24 detection. (B,F)
424 Histograms depicting representative staining with bnAbs (Green) and nnAbs (Black)
425 (C,G). Graphs shown represent the median fluorescence intensities (MFI) obtained for at
426 least 6 independent staining with the different mAbs. Error bars indicate means ± standard
427 errors of the means. (D,H) Graphs shown represent the mean MFI obtained with each
428 mAb. Statistical significance was tested using Mann-Whitney U test (** $p<0.01$, ns: non-
429 significant).

430

431 **Figure 2. Nef is expressed in HIV-1-infected cells undergoing CD4 downregulation**
432 **and expressing high levels of p24.**
433 Primary CD4+ T cells, mock-infected or infected with the transmitted-founder virus CH77,
434 either WT or defective for Nef expression (Nef-) were stained for cell-surface CD4 prior
435 detection of intracellular HIV-1 p24 and Nef expression. (A) Histograms depicting
436 representative intracellular Nef staining when gating on $CD4^{+}p24^{-}$, $CD4^{+}p24^{low}$ or
437 $CD4^{low}p24^{high}$ cells. In the context of cells infected with CH77TF Nef-, in the absence of
438 Nef-mediated CD4 downmodulation, the $p24^{high}$ remained $CD4^{high}$ ($CD4^{high}p24^{high}$). (B)
439 Quantification of the median fluorescence intensities (MFI) obtained for 6 independent
440 experiments. Error bars indicate means ± standard errors of the means. Statistical

441 significance was tested using multipe Mann-Withey tests with a Holm-Sidak post-test (**
442 p<0.01, ns: non-significant).
443
444 **Figure 3. HIV-1 late transcripts are mostly detected among cells that downregulated**
445 **CD4.** Purified primary CD4+ T cells, mock-infected or infected with the transmitted-founder
446 virus CH077 WT were stained for cell-surface CD4 prior detection of intracellular HIV-1
447 p24 and *env* mRNA and *nef* mRNA by RNA-flow FISH. (A) Representative example of
448 flow cytometry gating strategy based on cell-surface CD4 and intracellular p24 detection.
449 (B) Representative example of RNA-flow FISH detection of *env* and *nef* mRNA among the
450 different cell populations. (C) Quantification of the percentage of *env* mRNA+ *nef* mRNA+
451 cells detected among the different cell populations in three different donors. (D)
452 Alternatively, productively-infected cells were first identified based on *env* and *nef* mRNA
453 detection (E) Quantification of the percentage of $CD4^{+}p24^{-}$, $CD4^{+}p24^{low}$, $CD4^{low}p24^{low}$ and
454 $CD4^{low}p24^{high}$ cells among the *env* and *nef* mRNA+ cells with three different donors.
455 Statistical significance was tested using one-way ANOVA with a Holm-Sidak post-test
456 (****p<0.0001, ns: non-significant).
457
458 **Figure 4. Productively-infected cells are resistant to recognition by A32**.
459 Purified primary CD4+ T cells, mock-infected or infected with the transmitted-founder virus
460 CH077 WT were stained with A32 or PGT126, followed with appropriate secondary Abs.
461 Cells were then stained for cell-surface CD4 prior detection of intracellular HIV-1 p24 and
462 *Env* mRNA and *nef* mRNA by RNA-flow FISH. (A-C) In a first analysis, HIV-infected cells
463 were identified, then A32 and PGT126 binding was evaluated. (A) Example of RNA-flow
464 FISH gating strategy based on *env* and *nef* mRNA detection. (B) Example of antibody
465 binding among the *env/nef* mRNA- and *env/nef* mRNA+ cell population. (C) Quantification
466 of the percentage of cells recognized by either A32 or PGT126 among the *env/nef* mRNA-

467 and *env/nef* mRNA+ cell population with three different donors. (D-F) In a second
468 alternative analysis, Ab-binding cells were first identied, and the HIV-infection status was
469 then evaluated. (D) Example of flow cytometry gating strategy based on A32 or PGT126
470 binding. (E) Example of *env/nef* mRNA detection among the cells recognized (Ab+) or not
471 (Ab-) by indicated mAbs. (F) Quantification of the percentage of *env/nef* mRNA+ cells
472 among the cells recognized (Ab+) or not (Ab-) by indicated mAbs with three donors.
473 Statistical significance was tested using a two-way ANOVA with a Holm-Sidak post-test (*
474 $p<0.05$,** $p<0.01$, **** $p<0.0001$, ns: non-significant).
475
476 **Figure 5. *Ex vivo* expanded CD4+ T cells isolated from PLWH are preferentially**
477 **targeted by bNAbs.**
478 *Ex vivo* expanded CD4+ T cells from 6 PLWH were stained with bnAbs and nnAbs +/-
479 CD4mc, followed by appropriate secondary Abs. Cells were then stained for surface CD4
480 prior to detection of intracellular HIV-1 p24. (A) Percentage of p24+ upon activation
481 overtime. (B) Example of flow cytometry gating based on CD4 and p24 detection. (C)
482 Histograms depicting representative staining with bnAbs (Green) and nnAbs (Black). (D)
483 Median fluorescence intensities (MFI) obtained with 6 HIV+ individuals. (E) Graphs shown
484 represent the mean MFI obtained with each mAb. Each symbol represent a diffirent HIV+
485 donor. Statistical significance was tested using Mann-Whitney U test (* $p<0.05$, ****
486 $p<0.0001$).
487
488 **Figure 6. *Ex vivo* expanded CD4+ T cells isolated from PLWH are resistant to ADCC**
489 **mediated by nnAbs.**
490 *Ex vivo* expanded CD4 T cells from PLWH were used as target cells, while autologous
491 PBMC were used as effector cells in our FACS-based ADCC assays. (A) Graph shown
492 represent the percentage of ADCC against the $CD4^{low}p24^{high}$ cells with the single mAbs

493 and (B) nnAbs vs bnAbs. (A) Each symbol represent a diffirent HIV+ donor. Statistical
494 significance was tested using unpaired t test (**** p<0.0001).
495
496 **Figure 7. A32 nnAb does not impact viral replication or the size of the reservoir *in***
497 ***vivo***
498 (A) Experimental outline. NSG-15-Hu-PBL mice were infected with HIV-1 JRCSF
499 intraperitoneally. At day 6 and 9 post infection, mice were administered 1.5 mg of A32 or
500 3BNC117 (WT or GRLR) mAb subcutaneously (S.C.). (B) Mice were bled routinely for
501 plasma viral load (PVL) and flow cytometry analysis. PVL levels were measured by
502 quantitative real-time PCR (limit of detection = 300 copies/mL, dotted line). (C) Percentage
503 of CD4+ T cells in peripheral blood was evaluated by flow cytometry . At least six mice
504 were used for each treatment. (D-E) Tissues of JRCSF-infected NSG-15 hu-PBL mice,
505 treated or not with A32 or 3BNC117 (WT or GRLR) were harvested at day 11. (D)
506 Percentage of CD4+ T cells was evaluated by flow cytometry (E) CD4+ T cells were
507 isolated for real-time PCR analysis of HIV DNA. Each dot represents the mean values +/-
508 SEM. S.C., subcutaneous; I.P., intraperitoneal; BM, bone marrow; mock-treated = no
509 antibody. Statistical significance was tested using one way ANOVA with a Holm-Sidak
510 post-test or a Kruskal-Wallis test with a Dunn's post-test (* p<0.05,** p<0.01,*** p<0.001)

511 **METHODS**

512

513 **Ethics Statement**

514 Written informed consent was obtained from all study participants and research adhered
515 to the ethical guidelines of CRCHUM and was reviewed and approved by the CRCHUM
516 institutional review board (ethics committee, approval number MP-02-2024-11734).
517 Research adhered to the standards indicated by the Declaration of Helsinki. All
518 participants were adult and provided informed written consent prior to enrolment in
519 accordance with Institutional Review Board approval.

520

521 **Cell lines and primary cells**

522 293T human embryonic kidney cells (obtained from ATCC) were maintained at 37°C under
523 5% CO_2 in Dulbecco's Modified Eagle Medium (DMEM) (Wisent, St. Bruno, QC, Canada),
524 supplemented with 5% fetal bovine serum (FBS) (VWR, Radnor, PA, USA) and 100 U/mL
525 penicillin/streptomycin (Wisent). Human peripheral blood mononuclear cells (PBMCs)
526 from HIV-negative individuals and HIV-positive individuals obtained by leukapheresis and
527 Ficoll-Paque density gradient isolation were cryopreserved in liquid nitrogen until further
528 use. CD4+ T lymphocytes were purified from resting PBMCs by negative selection using
529 immunomagnetic beads per the manufacturer's instructions (StemCell Technologies,
530 Vancouver, BC) and were activated with phytohemagglutinin-L (10 µg/mL) for 48 h and
531 then maintained in RPMI 1640 (Thermo Fisher Scientific, Waltham, MA, USA) complete
532 medium supplemented with rIL-2 (100 U/mL).

533

534 **Antibody production**

535 FreeStyle 293F cells (Thermo Fisher Scientific) were grown in FreeStyle 293F medium
536 (Thermo Fisher Scientific) to a density of 1×10^6 cells/mL at 37°C with 8% CO_2 with regular

537 agitation (150 rpm). Cells were transfected with plasmids expressing the light and heavy
538 chains of each mAb using ExpiFectamine 293 transfection reagent, as directed by the
539 manufacturer (Thermo Fisher Scientific). One week later, the cells were pelleted and
540 discarded. The supernatants were filtered (0.22-μm-pore-size filter), and antibodies were
541 purified by protein A affinity columns, as directed by the manufacturer (Cytiva,
542 Marlborough, MA, USA).
543
544 **HIV-1 studies in humanized mice**
545 NSG-15 mice with expression of the human IL15 gene in the NOD/ShiLtJ background
546 were purchased from the Jackson Laboratory (Bar Harbor, ME, USA). The mice were bred
547 and maintained under specific pathogen-free conditions. All animal studies were
548 performed with authorization from Institutional Animal Care and Use Committees (IACUC)
549 of Yale University. NSG-15-Hu-PBL mice were engrafted as described (41). Briefly, 3.5 ×
550 10^6 PBMCs, purified by Ficoll density gradient centrifugation of healthy donor blood buffy
551 coats, obtained from the New York Blood Bank) were injected IP in a 200-μL volume into
552 6- to 8-week-old NSG-15 mice, using a 1-cm^3 syringe and 25-gauge needle. Cell
553 engraftment was tested 15 days post-transplant. 100 μL of blood was collected by
554 retroorbital bleeding. PBMCs were isolated by Ficoll density gradient centrifugation;
555 stained with fluorescently-labelled anti-human CD45 (BD Biosciences, Cat#: 555485) ,
556 CD3 (Biolegend, Cat#: 300424), CD4 (Biolegend, Cat#: 317432), CD8 (BD Biosciences,
557 Cat#: 561617) and CD56 (Biolegend, Cat#: 362508) antibodies and analyzed by flow
558 cytometry to confirm engraftment. Humanized mice were intraperitoneally challenged with
559 30,000 PFU of HIV-1_{JRCSF}. Infection profile was analyzed routinely by retro-orbital bleeding
560 and flow cytometric analysis of peripheral blood for human immune cells and PVL
561 analysis. For flow cytometry, 100 μl of blood was collected by retro-orbital bleeding at each
562 time point. PBMCs were isolated by Ficoll density gradient centrifugation and cells were

563 stained with fluor-conjugated antibodies as detailed above. PVL were measured at day 5,
564 8 and 11 post-infection, while HIV-1 reservoirs were measured at day 11 post-infected as
565 previously described (41).
566
567 **Plasmids and proviral constructs**
568 Transmitted/Founder (T/F) infectious molecular clone (IMC) of patient CH077 was inferred
569 and constructed as previously described (103). The generation of *nef*-defective CH077TF
570 was previously described and consists in the introduction of premature stop codons in the
571 *nef* reading frame using site-directed mutagenesis protocol (104). The CH077TF D368R
572 was also generated by site-directed mutagenesis as previously described (42). Proviral
573 constructs comprising an HIV-1 NL4.3-based isogenic backbone engineered for the
574 insertion of heterologous *env* strain sequences and expression in *cis* of full length Env
575 (Env-IMCs), were previously described (105). The Env-IMCs utilized in the present study
576 are those encoding Env form BaL (pNL-B.BaL.ecto), CH040 (pNL-B.CH040.ecto), CH058
577 (pNL-B.CH058.ecto), SF162 (pNL-B.SF162.ecto) or YU2 (pNL-B.YU-2.ecto). The proviral
578 plasmid pNL4.3 was used as control (106). The vesicular stomatitis virus G (VSV-G)-
579 encoding plasmid was previously described (107).
580
581 **Viral production, infections and *ex vivo* amplification.**
582 For *in vitro* infection, vesicular stomatitis virus G (VSV-G)-pseudotyped HIV-1 viruses
583 were produced by co-transfection of 293T cells with an HIV-1 proviral construct and a
584 VSV-G-encoding vector using the calcium phosphate method. Two days post-
585 transfection, cell supernatants were harvested, clarified by low-speed centrifugation (300
586 × g for 5 min), and concentrated by ultracentrifugation at 4°C (100,605 × g for 1 h) over
587 a 20% sucrose cushion. Pellets were resuspended in fresh RPMI, and aliquots were
588 stored at −80°C until use. Viruses were then used to infect activated primary CD4+ T cells

589 from healthy HIV-1 negative donors by spin infection at 800 × *g* for 1 h in 96-well plates
590 at 25 °C. Viral preparations were titrated directly on primary CD4+ T cells to achieve
591 similar levels of infection among the different IMCs tested (around 10% of p24+ cells). To
592 expand endogenously infected CD4+ T cells, primary CD4+ T cells obtained from PLWH
593 were isolated from PBMCs by negative selection. Purified CD4+ T cells were activated
594 with PHA-L at 10 µg/mL for 48 h and then cultured for at least 6 days in RPMI 1640
595 complete medium supplemented with rIL-2 (100 U/ml) to reach greater than 10% infection
596 for the ADCC assay.
597
598 **Antibodies**
599 The following anti-Env Abs were used to stained HIV-1-infected primary CD4+ T cells:
600 anti-gp41 ID F240; anti-cluster A A32, C11; anti-co-receptor binding site 17b; anti-gp120
601 outer domain 2G12, anti-CD4 binding site VRC03, 3BNC117; anti-V3 glycan PGT121,
602 PGT126, 10-1074; anti-V2 apex PG9; anti-gp120-gp41 interface PGT151. The HIV-IG
603 polyclonal antibody consists of anti-HIV immunoglobulins purified from a pool of plasma
604 from HIV+ asymptomatic donors (NIH AIDS Reagent Program). Goat anti-human IgG
605 (H+L) (Thermo Fisher Scientific) pre-coupled to Alexa Fluor 647 were used as secondary
606 antibodies in flow cytometry experiments. Rabbit antisera raised against Nef (NIH AIDS
607 Reagent Program) was used as primary antibodies in intracellular staining. BrillantViolet
608 421 (BV421)-conjugated donkey anti-rabbit antibodies (Biolegend) was used as
609 secondary antibodies to detect Nef antisera binding by flow cytometry. FITC or PE-
610 conjugated Mouse anti-human CD4 (clone OKT4; Biolegend) were used for cell-surface
611 staining of HIV-1-infected primary CD4+ T cells, while PE or FITC-conjugated Mouse anti-
612 HIV-1 p24 (clone KC57; Beckman coulter) were used for intracellular staining.
613
614 **Flow cytometry analysis of cell-surface staining**

615 Cell surface staining was performed at 48h post-infection. Mock-infected or HIV-1-infected
616 primary CD4+ T cells were incubated for 30 min at 37°C with anti-Env mAbs (5 µg/mL) or
617 HIV-IG (50 µg/mL). Cells were then washed once with PBS and stained with the
618 appropriate Alexa Fluor 647-conjugated secondary antibody (2 µg/mL) for 20 min at room
619 temperature. Cells were then stained with FITC- or PE-conjugated Mouse anti-CD4 Abs.
620 After two PBS washs, cells were fixed in a 2% PBS-formaldehyde solution. Infected cells
621 were then permeabilized using the Cytofix/Cytoperm Fixation/ Permeabilization Kit (BD
622 Biosciences, Mississauga, ON, Canada) and stained intracellularly using PE or FITC-
623 conjugated mouse anti-p24 mAb (clone KC57; Beckman Coulter, Brea, CA, USA; 1:100
624 dilution). The percentage of infected cells ($p24^{+}$) was determined by gating on the living
625 cell population according to a viability dye staining (Aqua Vivid; Thermo Fisher Scientific).
626 Alternatively, cells were stained intracellularly with rabbit antisera raised against Nef
627 (1:1000) followed by BV421-conjugated anti-rabbit secondary antibody. Samples were
628 acquired on an LSR II cytometer (BD Biosciences), and data analysis was performed
629 using FlowJo v10.5.3 (Tree Star, Ashland, OR, USA).
630

631 **Antibody-dependant cellular cytotoxicity (ADCC) assay**

632 Measurement of ADCC using a fluorescence-activated cell sorting (FACS)-based infected
633 cell elimination (ICE) assay was performed at 48 h post-infection. Briefly, HIV-1-infected
634 primary CD4+ T cells were stained with AquaVivid viability dye and cell proliferation dye
635 eFluor670 (Thermo Fisher Scientific) and used as target cells. Cryopreserved autologous
636 PBMC effectors cells, stained with cell proliferation dye eFluor450 (Thermo Fisher
637 Scientific), were added at an effector: target ratio of 10:1 in 96-well V-bottom plates
638 (Corning, Corning, NY). Anti-Env mAbs (5 µg/mL) was added to appropriate wells and
639 cells were incubated for 5 min at room temperature. The plates were subsequently

640 centrifuged for 1 min at 300 × g, and incubated at 37 °C, 5 % CO_2 for 5 h. before being
641 stained with FITC- or PE-conjugated Mouse anti-CD4 Abs. After one PBS wash, cells were
642 fixed in a 2% PBS-formaldehyde solution. Infected cells were then permeabilized using
643 the Cytofix/Cytoperm Fixation/ Permeabilization Kit (BD Biosciences, Mississauga, ON,
644 Canada) and stained intracellularly using PE or FITC-conjugated mouse anti-p24 mAb
645 (clone KC57; Beckman Coulter, Brea, CA, USA; 1:100 dilution) Productively-infected cells
646 were identified based on p24 and CD4 detection as described above. Samples were
647 acquired on an LSR II cytometer (BD Biosciences) and data analysis was performed using
648 FlowJo v10.5.3 (Tree Star). The percentage of ADCC was calculated with the following
649 formula: [(% of $CD4^+p24^{high}$ cells in Targets plus Effectors) − (% of $CD4^+p24^{high}$ cells in
650 Targets plus Effectors plus plasma or mAbs) / (% of $CD4^+p24^{high}$ cells in Targets) × 100]
651 by gating on infected lived target cells.
652
653 **RNAflow-FISH analysis.**
654 All buffers and fixation reagents were provided with the kit, with the exception of flow
655 cytometry staining buffer (2% FCS/PBS). The HIV-1 RNAflow-FISH assay was performed
656 as previously described and as per manufacturer's instructions (78-80). Briefly, cells were
657 harvested 48h post-infection and stained with the anti-Env mAbs A32 or PGT126 as
658 described above. Cells were then stained with Fixable Viability Dye (20 min, 4°C, Fixable
659 LiveDead, eBioscience) and then with a mix containing a brilliant stain buffer (BD
660 Biosciences) and the surface markers for CD4+ T cells detection (CD3 and CD4) and
661 CD8/NK/B cells and macrophages exclusions (CD8, CD56, CD19, CD16) (30 min, 4°C).
662 Samples were fixed, permeabilized with buffers provided by the manufacturer, and labeled
663 intracellularly for the structural HIV-1 p24 protein with the anti-p24 clone KC57 antibody
664 (30 min RT followed by 30 min 4°C, Beckman Coulter). HIV-1 RNA probing was performed

665 using the PrimeFlow RNA Assay (ThermoFisher). HIV-1 RNA were labeled using HIV-1
666 *env*RNA (Thermofisher; catalog number VF6-6000978) and HIV-1 *nef*RNA (Thermofisher;
667 catalog number (VF4-6000647) probe sets. HIV-1 *env*RNA was designed based on
668 CH077TF full env sequence, whereas HIV-1 *nef*RNA was based on consensus B HIV-1
669 sequence. Each probeset allows the hybridization of specific complementary branched
670 DNA nanostructure with different excitation/emission spectra. The probeset were diluted
671 1:5 in diluent and hybridized to the target mRNAs for 2 hr at 40°C. Samples were washed
672 to remove excess probes and stored overnight in the presence of RNAsin. Signal
673 amplification was achieved by performing sequential hybridization with DNA branches
674 (i.e., Pre-Amplifier and Amplifier) The first DNA branch in the Pre-Amplifier Mix was added
675 at a 1:1 ratio and was allowed to hybridize for 1.5 h at 40°C. Then the second DNA branch
676 in the Amplifier Mix was added and hybridized for 1.5 h at 40°C (78-80). Amplified mRNAs
677 were labeled with fluorescently tagged probes allowing hybridization for 1 hr at 40°C.
678 Samples were acquired on an LSRFortessa (BD Biosciences) and analyzed using FlowJo
679 (BD, V10.7.0). Unspecific binding of the fluorescent labeled branched probe in the
680 multiplex kit can lead to a low level of false-positive background noise, which, if present,
681 is detected across all the four channels corresponding to the types of labeled probes
682 (AF488, AF594, AF647, AF750). To decrease background noise, we thus left the AF594
683 channel vacant and excluded false-positive events based on fluorescence in this channel
684 before further gating. Gates were set on the HIV-uninfected donor control, or unstimulated
685 control where appropriate.
686

687 **QUANTIFICATION AND STATISTICAL ANALYSIS**

688 Statistics were analyzed using GraphPad Prism version 9.1.0 (GraphPad, San Diego, CA,
689 USA). Every data set was tested for statistical normality and this information was used to
690 apply the appropriate (parametric or nonparametric) statistical test. P values <0.05 were

691 considered significant; significance values are indicated as * $P<0.05$, ** $P<0.01$, ***
692 $P<0.001$, **** $P<0.0001$.
693
694 **Data availability**
695 The published article includes all datasets generated and analyzed for this study. Further
696 information and requests for resources and reagents should be directed to and will be
697 fulfilled by the Lead Contact Author (andres.finzi@umontreal.ca). All unique reagents
698 generated in this study are available from the Lead Contact with a completed Materials
699 Transfer Agreement.

700 **REFERENCES**

701 1. Antiretroviral Therapy Cohort C. Life expectancy of individuals on combination
702 antiretroviral therapy in high-income countries: a collaborative analysis of 14
703 cohort studies. *Lancet.* 2008;372(9635):293-9.
704 2. Deeks SG, Lewin SR, and Havlir DV. The end of AIDS: HIV infection as a chronic
705 disease. *Lancet.* 2013;382(9903):1525-33.
706 3. Finzi D, Hermankova M, Pierson T, Carruth LM, Buck C, Chaisson RE, et al.
707 Identification of a reservoir for HIV-1 in patients on highly active antiretroviral
708 therapy. *Science.* 1997;278(5341):1295-300.
709 4. Chomont N, El-Far M, Ancuta P, Trautmann L, Procopio FA, Yassine-Diab B, et al.
710 HIV reservoir size and persistence are driven by T cell survival and homeostatic
711 proliferation. *Nat Med.* 2009;15(8):893-900.
712 5. Chun TW, Stuyver L, Mizell SB, Ehler LA, Mican JA, Baseler M, et al. Presence of an
713 inducible HIV-1 latent reservoir during highly active antiretroviral therapy. *Proc*
714 *Natl Acad Sci U S A.* 1997;94(24):13193-7.
715 6. Chun TW, Carruth L, Finzi D, Shen X, DiGiuseppe JA, Taylor H, et al. Quantification
716 of latent tissue reservoirs and total body viral load in HIV-1 infection. *Nature.*
717 1997;387(6629):183-8.
718 7. Checkley MA, Luttge BG, and Freed EO. HIV-1 envelope glycoprotein biosynthesis,
719 trafficking, and incorporation. *J Mol Biol.* 2011;410(4):582-608.
720 8. Frattari GS, Caskey M, and Sogaard OS. Broadly neutralizing antibodies for HIV
721 treatment and cure approaches. *Curr Opin HIV AIDS.* 2023;18(4):157-63.
722 9. Bar KJ, Sneller MC, Harrison LJ, Justement JS, Overton ET, Petrone ME, et al. Effect
723 of HIV Antibody VRC01 on Viral Rebound after Treatment Interruption. *N Engl J*
724 *Med.* 2016;375(21):2037-50.
725 10. Caskey M, Klein F, Lorenzi JC, Seaman MS, West AP, Jr., Buckley N, et al. Viraemia
726 suppressed in HIV-1-infected humans by broadly neutralizing antibody 3BNC117.
727 *Nature.* 2015;522(7557):487-91.
728 11. Caskey M, Schoofs T, Gruell H, Settler A, Karagounis T, Kreider EF, et al. Antibody
729 10-1074 suppresses viremia in HIV-1-infected individuals. *Nat Med.*
730 2017;23(2):185-91.
731 12. Lynch RM, Boritz E, Coates EE, DeZure A, Madden P, Costner P, et al. Virologic
732 effects of broadly neutralizing antibody VRC01 administration during chronic HIV-
733 1 infection. *Science translational medicine.* 2015;7(319):319ra206.
734 13. Scheid JF, Horwitz JA, Bar-On Y, Kreider EF, Lu CL, Lorenzi JC, et al. HIV-1 antibody
735 3BNC117 suppresses viral rebound in humans during treatment interruption.
736 *Nature.* 2016;535(7613):556-60.
737 14. Gaebler C, Nogueira L, Stoffel E, Oliveira TY, Breton G, Millard KG, et al. Prolonged
738 viral suppression with anti-HIV-1 antibody therapy. *Nature.* 2022;606(7913):368-
739 74.
740 15. Mendoza P, Gruell H, Nogueira L, Pai JA, Butler AL, Millard K, et al. Combination
741 therapy with anti-HIV-1 antibodies maintains viral suppression. *Nature.*
742 2018;561(7724):479-84.

743 16. Thali M, Moore JP, Furman C, Charles M, Ho DD, Robinson J, and Sodroski J.
744 Characterization of conserved human immunodeficiency virus type 1 gp120
745 neutralization epitopes exposed upon gp120-CD4 binding. *J Virol.*
746 1993;67(7):3978-88.
747 17. Kwong PD, Wyatt R, Robinson J, Sweet RW, Sodroski J, and Hendrickson WA.
748 Structure of an HIV gp120 envelope glycoprotein in complex with the CD4 receptor
749 and a neutralizing human antibody. *Nature.* 1998;393(6686):648-59.
750 18. Wyatt R, Kwong PD, Desjardins E, Sweet RW, Robinson J, Hendrickson WA, and
751 Sodroski JG. The antigenic structure of the HIV gp120 envelope glycoprotein.
752 *Nature.* 1998;393(6686):705-11.
753 19. Tolbert WD, Gohain N, Veillette M, Chapleau JP, Orlandi C, Visciano ML, et al.
754 Paring Down HIV Env: Design and Crystal Structure of a Stabilized Inner Domain of
755 HIV-1 gp120 Displaying a Major ADCC Target of the A32 Region. *Structure.*
756 2016;24(5):697-709.
757 20. Tolbert WD, Gohain N, Alsahafi N, Van V, Orlandi C, Ding S, et al. Targeting the
758 Late Stage of HIV-1 Entry for Antibody-Dependent Cellular Cytotoxicity: Structural
759 Basis for Env Epitopes in the C11 Region. *Structure.* 2017;25(11):1719-31 e4.
760 21. Gohain N, Tolbert WD, Acharya P, Yu L, Liu T, Zhao P, et al. Cocrystal Structures of
761 Antibody N60-i3 and Antibody JR4 in Complex with gp120 Define More Cluster A
762 Epitopes Involved in Effective Antibody-Dependent Effector Function against HIV-
763 1. *J Virol.* 2015;89(17):8840-54.
764 22. Gohain N, Tolbert WD, Orlandi C, Richard J, Ding S, Chen X, et al. Molecular basis
765 for epitope recognition by non-neutralizing anti-gp41 antibody F240. *Scientific*
766 *reports.* 2016;6:36685.
767 23. Veillette M, Coutu M, Richard J, Batraville LA, Dagher O, Bernard N, et al. The HIV-
768 1 gp120 CD4-bound conformation is preferentially targeted by antibody-
769 dependent cellular cytotoxicity-mediating antibodies in sera from HIV-1-infected
770 individuals. *J Virol.* 2015;89(1):545-51.
771 24. Prevost J, Anand SP, Rajashekar JK, Zhu L, Richard J, Goyette G, et al. HIV-1 Vpu
772 restricts Fc-mediated effector functions in vivo. *Cell reports.* 2022;41(6):111624.
773 25. Decker JM, Bibollet-Ruche F, Wei X, Wang S, Levy DN, Wang W, et al. Antigenic
774 conservation and immunogenicity of the HIV coreceptor binding site. *The Journal*
775 *of experimental medicine.* 2005;201(9):1407-19.
776 26. Veillette M, Desormeaux A, Medjahed H, Gharsallah NE, Coutu M, Baalwa J, et al.
777 Interaction with cellular CD4 exposes HIV-1 envelope epitopes targeted by
778 antibody-dependent cell-mediated cytotoxicity. *J Virol.* 2014;88(5):2633-44.
779 27. Richard J, Pacheco B, Gohain N, Veillette M, Ding S, Alsahafi N, et al. Co-receptor
780 Binding Site Antibodies Enable CD4-Mimetics to Expose Conserved Anti-cluster A
781 ADCC Epitopes on HIV-1 Envelope Glycoproteins. *EBioMedicine.* 2016;12:208-18.
782 28. Ferrari G, Pollara J, Kozink D, Harms T, Drinker M, Freel S, et al. An HIV-1 gp120
783 envelope human monoclonal antibody that recognizes a C1 conformational
784 epitope mediates potent antibody-dependent cellular cytotoxicity (ADCC) activity
785 and defines a common ADCC epitope in human HIV-1 serum. *J Virol.*
786 2011;85(14):7029-36.

787 29. Munro JB, Gorman J, Ma X, Zhou Z, Arthos J, Burton DR, et al. Conformational
788 dynamics of single HIV-1 envelope trimers on the surface of native virions. *Science.*
789 2014;346(6210):759-63.
790 30. Ma X, Lu M, Gorman J, Terry DS, Hong X, Zhou Z, et al. HIV-1 Env trimer opens
791 through an asymmetric intermediate in which individual protomers adopt distinct
792 conformations. *eLife.* 2018;7.
793 31. Herschhorn A, Ma X, Gu C, Ventura JD, Castillo-Menendez L, Melillo B, et al.
794 Release of gp120 Restraints Leads to an Entry-Competent Intermediate State of
795 the HIV-1 Envelope Glycoproteins. *MBio.* 2016;7(5):doi:10.1128/mBio.01598-16.
796 32. von Bredow B, Arias JF, Heyer LN, Moldt B, Le K, Robinson JE, et al. Comparison of
797 Antibody-Dependent Cell-Mediated Cytotoxicity and Virus Neutralization by HIV-
798 1 Env-Specific Monoclonal Antibodies. *J Virol.* 2016;90(13):6127-39.
799 33. Richard J, Prevost J, Baxter AE, von Bredow B, Ding S, Medjahed H, et al.
800 Uninfected Bystander Cells Impact the Measurement of HIV-Specific Antibody-
801 Dependent Cellular Cytotoxicity Responses. *mBio.* 2018;9(2).
802 34. Ding S, Veillette M, Coutu M, Prevost J, Scharf L, Bjorkman PJ, et al. A Highly
803 Conserved Residue of the HIV-1 gp120 Inner Domain Is Important for Antibody-
804 Dependent Cellular Cytotoxicity Responses Mediated by Anti-cluster A Antibodies.
805 *J Virol.* 2015;90(4):2127-34.
806 35. Bruel T, Guivel-Benhassine F, Lorin V, Lortat-Jacob H, Baleux F, Bourdic K, et al.
807 Lack of ADCC Breadth of Human Nonneutralizing Anti-HIV-1 Antibodies. *J Virol.*
808 2017;91(8):e02440-16.
809 36. Prevost J, Richard J, Ding S, Pacheco B, Charlebois R, Hahn BH, et al. Envelope
810 glycoproteins sampling states 2/3 are susceptible to ADCC by sera from HIV-1-
811 infected individuals. *Virology.* 2018;515:38-45.
812 37. Alsahafi N, Ding S, Richard J, Markle T, Brassard N, Walker B, et al. Nef Proteins
813 from HIV-1 Elite Controllers Are Inefficient at Preventing Antibody-Dependent
814 Cellular Cytotoxicity. *J Virol.* 2015;90(6):2993-3002.
815 38. Richard J, Veillette M, Brassard N, Iyer SS, Roger M, Martin L, et al. CD4 mimetics
816 sensitize HIV-1-infected cells to ADCC. *Proc Natl Acad Sci U S A.*
817 2015;112(20):E2687-94.
818 39. Prevost J, Richard J, Medjahed H, Alexander A, Jones J, Kappes JC, et al. Incomplete
819 Downregulation of CD4 Expression Affects HIV-1 Env Conformation and Antibody-
820 Dependent Cellular Cytotoxicity Responses. *J Virol.* 2018;92(13).
821 40. Alsahafi N, Bakouche N, Kazemi M, Richard J, Ding S, Bhattacharyya S, et al. An
822 Asymmetric Opening of HIV-1 Envelope Mediates Antibody-Dependent Cellular
823 Cytotoxicity. *Cell Host Microbe.* 2019;25(4):578-87 e5.
824 41. Rajashekar JK, Richard J, Beloor J, Prevost J, Anand SP, Beaudoin-Bussieres G, et
825 al. Modulating HIV-1 envelope glycoprotein conformation to decrease the HIV-1
826 reservoir. *Cell Host Microbe.* 2021;29(6):904-16 e6.
827 42. Laumaea A, Marchitto L, Ding S, Beaudoin-Bussieres G, Prevost J, Gasser R, et al.
828 Small CD4 mimetics sensitize HIV-1-infected macrophages to antibody-dependent
829 cellular cytotoxicity. *Cell reports.* 2023;42(1):111983.

830 43. Herschhorn A, Gu C, Moraca F, Ma X, Farrell M, Smith AB, 3rd, et al. The beta20-
831 beta21 of gp120 is a regulatory switch for HIV-1 Env conformational transitions.
832 *Nat Commun.* 2017;8(1):1049.
833 44. Kwon YD, Finzi A, Wu X, Dogo-Isonagie C, Lee LK, Moore LR, et al. Unliganded HIV-
834 1 gp120 core structures assume the CD4-bound conformation with regulation by
835 quaternary interactions and variable loops. *Proc Natl Acad Sci U S A.*
836 2012;109(15):5663-8.
837 45. Alvarez RA, Hamlin RE, Monroe A, Moldt B, Hotta MT, Rodriguez Caprio G, et al.
838 HIV-1 Vpu antagonism of tetherin inhibits antibody-dependent cellular cytotoxic
839 responses by natural killer cells. *J Virol.* 2014;88(11):6031-46.
840 46. Arias JF, Heyer LN, von Bredow B, Weisgrau KL, Moldt B, Burton DR, et al. Tetherin
841 antagonism by Vpu protects HIV-infected cells from antibody-dependent cell-
842 mediated cytotoxicity. *Proc Natl Acad Sci U S A.* 2014;111(17):6425-30.
843 47. Veillette M, Coutu M, Richard J, Batraville LA, Desormeaux A, Roger M, and Finzi
844 A. Conformational evaluation of HIV-1 trimeric envelope glycoproteins using a
845 cell-based ELISA assay. *Journal of visualized experiments : JoVE.* 2014(91):51995.
846 48. Pauthner MG, Nkolola JP, Havenar-Daughton C, Murrell B, Reiss SM, Bastidas R, et
847 al. Vaccine-Induced Protection from Homologous Tier 2 SHIV Challenge in
848 Nonhuman Primates Depends on Serum-Neutralizing Antibody Titers. *Immunity.*
849 2019;50(1):241-52 e6.
850 49. Bonsignori M, Pollara J, Moody MA, Alpert MD, Chen X, Hwang KK, et al. Antibody-
851 Dependent Cellular Cytotoxicity-Mediating Antibodies from an HIV-1 Vaccine
852 Efficacy Trial Target Multiple Epitopes and Preferentially Use the VH1 Gene Family.
853 *J Virol.* 2012;86(21):11521-32.
854 50. Costa MR, Pollara J, Edwards RW, Seaman MS, Gorny MK, Montefiori DC, et al. Fc
855 Receptor-Mediated Activities of Env-Specific Human Monoclonal Antibodies
856 Generated from Volunteers Receiving the DNA Prime-Protein Boost HIV Vaccine
857 DP6-001. *J Virol.* 2016;90(22):10362-78.
858 51. Easterhoff D, Pollara J, Luo K, Tolbert WD, Young B, Mielke D, et al. Boosting with
859 AIDSVAX B/E Enhances Env Constant Region 1 and 2 Antibody-Dependent Cellular
860 Cytotoxicity Breadth and Potency. *J Virol.* 2020;94(4).
861 52. Fisher L, Zinter M, Stanfield-Oakley S, Carpp LN, Edwards RW, Denny T, et al.
862 Vaccine-Induced Antibodies Mediate Higher Antibody-Dependent Cellular
863 Cytotoxicity After Interleukin-15 Pretreatment of Natural Killer Effector Cells.
864 *Front Immunol.* 2019;10:2741.
865 53. Huang Y, Ferrari G, Alter G, Forthal DN, Kappes JC, Lewis GK, et al. Diversity of
866 Antiviral IgG Effector Activities Observed in HIV-Infected and Vaccinated Subjects.
867 *J Immunol.* 2016;197(12):4603-12.
868 54. Mielke D, Bandawe G, Zheng J, Jones J, Abrahams MR, Bekker V, et al. ADCC-
869 mediating non-neutralizing antibodies can exert immune pressure in early HIV-1
870 infection. *PLoS Pathog.* 2021;17(11):e1010046.
871 55. Mielke D, Stanfield-Oakley S, Borate B, Fisher LH, Faircloth K, Tuyishime M, et al.
872 Selection of HIV Envelope Strains for Standardized Assessments of Vaccine-Elicited

873 Antibody-Dependent Cellular Cytotoxicity-Mediating Antibodies. *J Virol.*
874 2022;96(2):e0164321.
875 56. Pollara J, Bonsignori M, Moody MA, Liu P, Alam SM, Hwang KK, et al. HIV-1 vaccine-
876 induced C1 and V2 Env-specific antibodies synergize for increased antiviral
877 activities. *J Virol.* 2014;88(14):7715-26.
878 57. Shubin Z, Stanfield-Oakley S, Puangkaew J, Pitisutthithum P, Nitayaphan S,
879 Gurunathan S, et al. Additional boosting to the RV144 vaccine regimen increased
880 Fc-mediated effector function magnitude but not durability. *AIDS.*
881 2023;37(10):1519-24.
882 58. Tuyishime M, Garrido C, Jha S, Moeser M, Mielke D, LaBranche C, et al. Improved
883 killing of HIV-infected cells using three neutralizing and non-neutralizing
884 antibodies. *J Clin Invest.* 2020;130(10):5157-70.
885 59. Williams LD, Shen X, Sawant SS, Akapirat S, Dahora LC, Tay MZ, et al. Viral vector
886 delivered immunogen focuses HIV-1 antibody specificity and increases durability
887 of the circulating antibody recall response. *PLoS Pathog.* 2023;19(5):e1011359.
888 60. Bradley T, Pollara J, Santra S, Vandergrift N, Pittala S, Bailey-Kellogg C, et al.
889 Pentavalent HIV-1 vaccine protects against simian-human immunodeficiency virus
890 challenge. *Nat Commun.* 2017;8:15711.
891 61. Prevost J, Richard J, Gasser R, Medjahed H, Kirchhoff F, Hahn BH, et al. Detection
892 of the HIV-1 Accessory Proteins Nef and Vpu by Flow Cytometry Represents a New
893 Tool to Study Their Functional Interplay within a Single Infected CD4(+) T Cell. *J*
894 *Virol.* 2022;96(6):e0192921.
895 62. Alberti MO, Jones JJ, Miglietta R, Ding H, Bakshi RK, Edmonds TG, et al. Optimized
896 Replicating Renilla Luciferase Reporter HIV-1 Utilizing Novel Internal Ribosome
897 Entry Site Elements for Native Nef Expression and Function. *AIDS Res Hum*
898 *Retroviruses.* 2015;31(12):1278-96.
899 63. Klotman ME, Kim S, Buchbinder A, DeRossi A, Baltimore D, and Wong-Staal F.
900 Kinetics of expression of multiply spliced RNA in early human immunodeficiency
901 virus type 1 infection of lymphocytes and monocytes. *Proc Natl Acad Sci U S A.*
902 1991;88(11):5011-5.
903 64. Kim SY, Byrn R, Groopman J, and Baltimore D. Temporal aspects of DNA and RNA
904 synthesis during human immunodeficiency virus infection: evidence for
905 differential gene expression. *J Virol.* 1989;63(9):3708-13.
906 65. Richard J, Prevost J, Bourassa C, Brassard N, Boutin M, Benlarbi M, et al. Temsavir
907 blocks the immunomodulatory activities of HIV-1 soluble gp120. *Cell Chem Biol.*
908 2023;30(5):540-52 e6.
909 66. Richard J, Veillette M, Ding S, Zoubchenok D, Alsahafi N, Coutu M, et al. Small CD4
910 Mimetics Prevent HIV-1 Uninfected Bystander CD4 + T Cell Killing Mediated by
911 Antibody-dependent Cell-mediated Cytotoxicity. *EBioMedicine.* 2016;3:122-34.
912 67. Brand D, Srinivasan K, and Sodroski J. Determinants of human immunodeficiency
913 virus type 1 entry in the CDR2 loop of the CD4 glycoprotein. *J Virol.*
914 1995;69(1):166-71.

915 68. Sloan DD, Lam CY, Irrinki A, Liu L, Tsai A, Pace CS, et al. Targeting HIV Reservoir in
916 Infected CD4 T Cells by Dual-Affinity Re-targeting Molecules (DARTs) that Bind HIV
917 Envelope and Recruit Cytotoxic T Cells. *PLoS Pathog.* 2015;11(11):e1005233.
918 69. Garrido C, Abad-Fernandez M, Tuyishime M, Pollara JJ, Ferrari G, Soriano-Sarabia
919 N, and Margolis DM. Interleukin-15-Stimulated Natural Killer Cells Clear HIV-1-
920 Infected Cells following Latency Reversal Ex Vivo. *J Virol.* 2018;92(12).
921 70. Grau-Exposito J, Serra-Peinado C, Miguel L, Navarro J, Curran A, Burgos J, et al. A
922 Novel Single-Cell FISH-Flow Assay Identifies Effector Memory CD4(+) T cells as a
923 Major Niche for HIV-1 Transcription in HIV-Infected Patients. *mBio.* 2017;8(4).
924 71. Mielke D, Bandawe G, Pollara J, Abrahams MR, Nyanhete T, Moore PL, et al.
925 Antibody-Dependent Cellular Cytotoxicity (ADCC)-Mediating Antibodies Constrain
926 Neutralizing Antibody Escape Pathway. *Front Immunol.* 2019;10:2875.
927 72. Orlandi C, Flinko R, and Lewis GK. A new cell line for high throughput HIV-specific
928 antibody-dependent cellular cytotoxicity (ADCC) and cell-to-cell virus transmission
929 studies. *J Immunol Methods.* 2016;433:51-8.
930 73. Richard J, Prevost J, Alsahafi N, Ding S, and Finzi A. Impact of HIV-1 Envelope
931 Conformation on ADCC Responses. *Trends in microbiology.* 2018;26(4):253-65.
932 74. Veillette M, Richard J, and Finzi A. Uncovering HIV-1-infected cells. *Oncotarget.*
933 2015.
934 75. Astorga-Gamaza A, Grau-Exposito J, Burgos J, Navarro J, Curran A, Planas B, et al.
935 Identification of HIV-reservoir cells with reduced susceptibility to antibody-
936 dependent immune response. *Elife.* 2022;11.
937 76. Pollara J, Hart L, Brewer F, Pickeral J, Packard BZ, Hoxie JA, et al. High-throughput
938 quantitative analysis of HIV-1 and SIV-specific ADCC-mediating antibody
939 responses. *Cytometry Part A : the journal of the International Society for Analytical*
940 *Cytology.* 2011;79(8):603-12.
941 77. Santra S, Tomaras GD, Warrier R, Nicely NI, Liao HX, Pollara J, et al. Human Non-
942 neutralizing HIV-1 Envelope Monoclonal Antibodies Limit the Number of Founder
943 Viruses during SHIV Mucosal Infection in Rhesus Macaques. *PLoS Pathog.*
944 2015;11(8):e1005042.
945 78. Baxter AE, Niessl J, Fromentin R, Richard J, Porichis F, Charlebois R, et al. Single-
946 Cell Characterization of Viral Translation-Competent Reservoirs in HIV-Infected
947 Individuals. *Cell Host Microbe.* 2016;20(3):368-80.
948 79. Baxter AE, Niessl J, Fromentin R, Richard J, Porichis F, Massanella M, et al.
949 Multiparametric characterization of rare HIV-infected cells using an RNA-flow FISH
950 technique. *Nature protocols.* 2017;12(10):2029-49.
951 80. Sannier G, Dube M, Dufour C, Richard C, Brassard N, Delgado GG, et al. Combined
952 single-cell transcriptional, translational, and genomic profiling reveals HIV-1
953 reservoir diversity. *Cell Rep.* 2021;36(9):109643.
954 81. Mengistu M, Ray K, Lewis GK, and DeVico AL. Antigenic properties of the human
955 immunodeficiency virus envelope glycoprotein gp120 on virions bound to target
956 cells. *PLoS Pathog.* 2015;11(3):e1004772.

957 82. Abeynaike SA, Huynh TR, Mehmood A, Kim T, Frank K, Gao K, et al. Human
958 Hematopoietic Stem Cell Engrafted IL-15 Transgenic NSG Mice Support Robust NK
959 Cell Responses and Sustained HIV-1 Infection. *Viruses.* 2023;15(2).
960 83. Bournazos S, Klein F, Pietzsch J, Seaman MS, Nussenzweig MC, and Ravetch JV.
961 Broadly neutralizing anti-HIV-1 antibodies require Fc effector functions for in vivo
962 activity. *Cell.* 2014;158(6):1243-53.
963 84. Guan Y, Pazgier M, Sajadi MM, Kamin-Lewis R, Al-Darmarki S, Flinko R, et al.
964 Diverse specificity and effector function among human antibodies to HIV-1
965 envelope glycoprotein epitopes exposed by CD4 binding. *Proc Natl Acad Sci U S A.*
966 2013;110(1):E69-78.
967 85. Robinson JE, Elliott DH, Martin EA, Micken K, and Rosenberg ES. High frequencies
968 of antibody responses to CD4 induced epitopes in HIV infected patients started on
969 HAART during acute infection. *Human antibodies.* 2005;14(3-4):115-21.
970 86. Wildum S, Schindler M, Munch J, and Kirchhoff F. Contribution of Vpu, Env, and
971 Nef to CD4 down-modulation and resistance of human immunodeficiency virus
972 type 1-infected T cells to superinfection. *J Virol.* 2006;80(16):8047-59.
973 87. Piguet V, Schwartz O, Le Gall S, and Trono D. The downregulation of CD4 and MHC-
974 I by primate lentiviruses: a paradigm for the modulation of cell surface receptors.
975 *Immunological reviews.* 1999;168:51-63.
976 88. Bresnahan PA, Yonemoto W, Ferrell S, Williams-Herman D, Geleziunas R, and
977 Greene WC. A dileucine motif in HIV-1 Nef acts as an internalization signal for CD4
978 downregulation and binds the AP-1 clathrin adaptor. *Curr Biol.* 1998;8(22):1235-
979 8.
980 89. Craig HM, Pandori MW, and Guatelli JC. Interaction of HIV-1 Nef with the cellular
981 dileucine-based sorting pathway is required for CD4 down-regulation and optimal
982 viral infectivity. *Proc Natl Acad Sci U S A.* 1998;95(19):11229-34.
983 90. Greenberg M, DeTulleo L, Rapoport I, Skowronski J, and Kirchhausen T. A dileucine
984 motif in HIV-1 Nef is essential for sorting into clathrin-coated pits and for
985 downregulation of CD4. *Curr Biol.* 1998;8(22):1239-42.
986 91. Mangasarian A, Foti M, Aiken C, Chin D, Carpentier JL, and Trono D. The HIV-1 Nef
987 protein acts as a connector with sorting pathways in the Golgi and at the plasma
988 membrane. *Immunity.* 1997;6(1):67-77.
989 92. Schwartz S, Felber BK, Fenyo EM, and Pavlakis GN. Env and Vpu proteins of human
990 immunodeficiency virus type 1 are produced from multiple bicistronic mRNAs. *J*
991 *Virol.* 1990;64(11):5448-56.
992 93. Geleziunas R, Bour S, and Wainberg MA. Cell surface down-modulation of CD4
993 after infection by HIV-1. *FASEB J.* 1994;8(9):593-600.
994 94. Willey RL, Maldarelli F, Martin MA, and Strebel K. Human immunodeficiency virus
995 type 1 Vpu protein induces rapid degradation of CD4. *J Virol.* 1992;66(12):7193-
996 200.
997 95. Willey RL, Maldarelli F, Martin MA, and Strebel K. Human immunodeficiency virus
998 type 1 Vpu protein regulates the formation of intracellular gp160-CD4 complexes.
999 *J Virol.* 1992;66(1):226-34.

1000 96. Wang S, Yates NL, Pollara J, Voronin Y, Stanfield-Oakley S, Han D, et al. Broadly
1001 binding and functional antibodies and persisting memory B cells elicited by HIV
1002 vaccine PDPHV. *NPJ Vaccines.* 2022;7(1):18.
1003 97. Chen BK, Gandhi RT, and Baltimore D. CD4 down-modulation during infection of
1004 human T cells with human immunodeficiency virus type 1 involves independent
1005 activities of vpu, env, and nef. *J Virol.* 1996;70(9):6044-53.
1006 98. Pollara J, Orlandi C, Beck C, Edwards RW, Hu Y, Liu S, et al. Application of area
1007 scaling analysis to identify natural killer cell and monocyte involvement in the
1008 GranToxiLux antibody dependent cell-mediated cytotoxicity assay. *Cytometry A.*
1009 2018;93(4):436-47.
1010 99. Chung AW, Navis M, Isitman G, Wren L, Silvers J, Amin J, et al. Activation of NK
1011 cells by ADCC antibodies and HIV disease progression. *J Acquir Immune Defic*
1012 *Syndr.* 2011;58(2):127-31.
1013 100. Yucha R, Litchford ML, Fish CS, Yaffe ZA, Richardson BA, Maleche-Obimbo E, et al.
1014 Higher HIV-1 Env gp120-Specific Antibody-Dependent Cellular Cytotoxicity (ADCC)
1015 Activity Is Associated with Lower Levels of Defective HIV-1 Provirus. *Viruses.*
1016 2023;15(10).
1017 101. Tomescu C, Kroll K, Colon K, Papasavvas E, Frank I, Tebas P, et al. Identification of
1018 the predominant human NK cell effector subset mediating ADCC against HIV-
1019 infected targets coated with BNAbs or plasma from PLWH. *Eur J Immunol.*
1020 2021;51(8):2051-61.
1021 102. Madani N, Princiotto AM, Mach L, Ding S, Prevost J, Richard J, et al. A CD4-mimetic
1022 compound enhances vaccine efficacy against stringent immunodeficiency virus
1023 challenge. *Nat Commun.* 2018;9(1):2363.
1024 103. Ochsenbauer C, Edmonds TG, Ding H, Keele BF, Decker J, Salazar MG, et al.
1025 Generation of Transmitted/Founder HIV-1 Infectious Molecular Clones and
1026 Characterization of Their Replication Capacity in CD4 T Lymphocytes and
1027 Monocyte-Derived Macrophages. *J Virol.* 2012;86(5):2715-28.
1028 104. van Stigt Thans T, Akko JI, Niehrs A, Garcia-Beltran WF, Richert L, Sturzel CM, et al.
1029 Primary HIV-1 Strains Use Nef To Downmodulate HLA-E Surface Expression. *J Virol.*
1030 2019;93(20).
1031 105. Edmonds TG, Ding H, Yuan X, Wei Q, Smith KS, Conway JA, et al. Replication
1032 competent molecular clones of HIV-1 expressing Renilla luciferase facilitate the
1033 analysis of antibody inhibition in PBMC. *Virology.* 2010;408(1):1-13.
1034 106. Adachi A, Gendelman HE, Koenig S, Folks T, Willey R, Rabson A, and Martin MA.
1035 Production of acquired immunodeficiency syndrome-associated retrovirus in
1036 human and nonhuman cells transfected with an infectious molecular clone. *J Virol.*
1037 1986;59(2):284-91.
1038 107. Emi N, Friedmann T, and Yee JK. Pseudotype formation of murine leukemia virus
1039 with the G protein of vesicular stomatitis virus. *J Virol.* 1991;65(3):1202-7.
1040

Graphical abstract

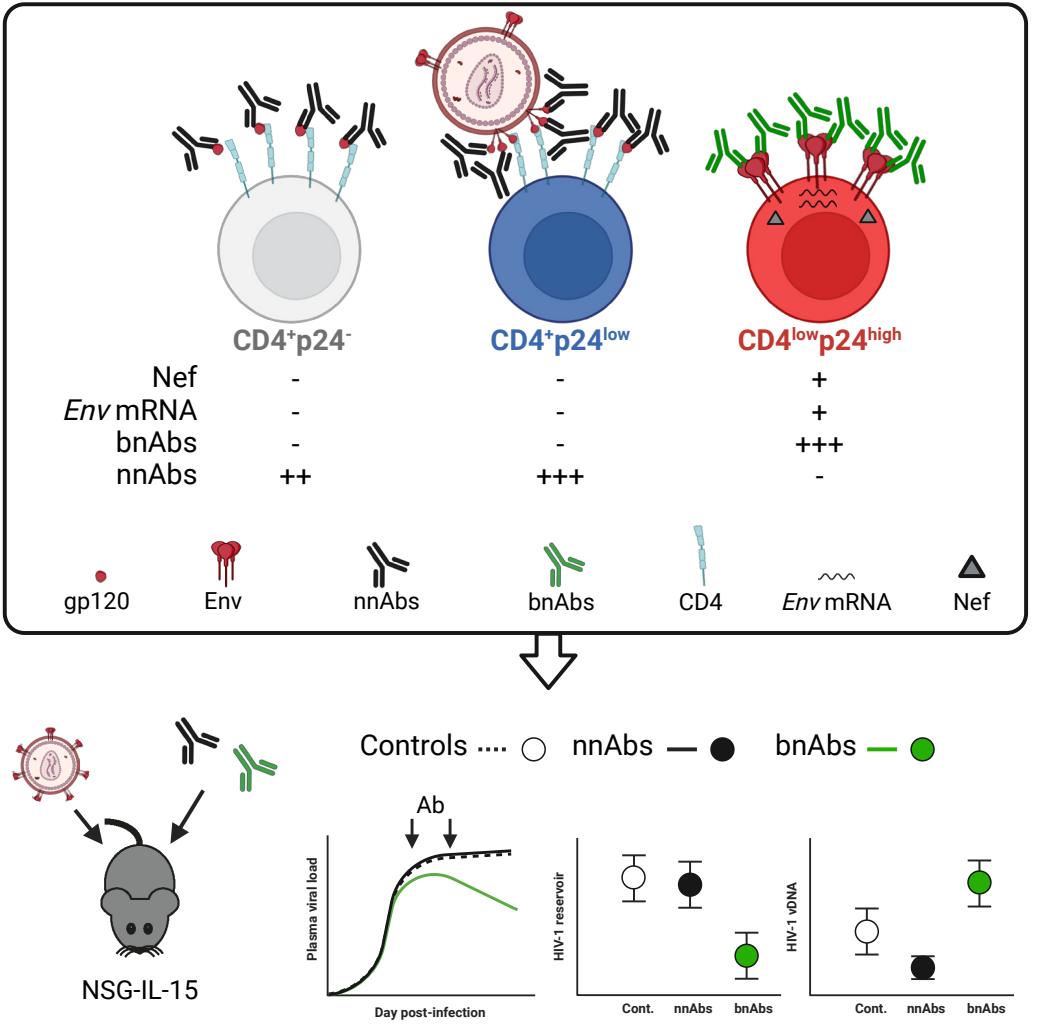

Figure 1

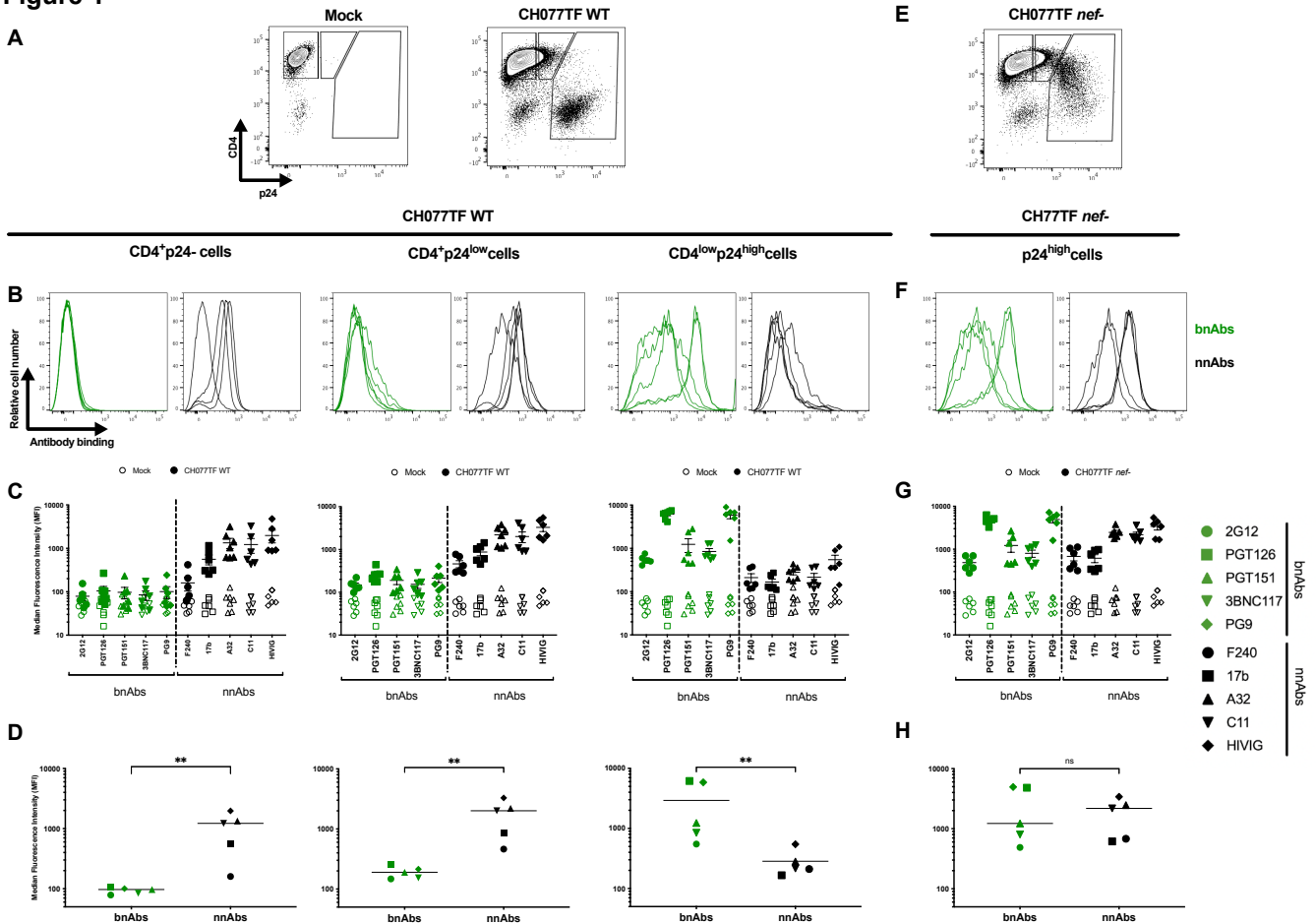
A
Mock
CH077TF WT
CD4
p24
E
CH077TF nef-
CH077TF WT
CH77TF nef-
CD4+p24- cells
CD4+p24low cells
CD4lowp24high cells
p24high cells
B
Relative cell number
Antibody binding
F
bnAbs
nnAbs
Mock
CH077TF WT
CH077TF nef-
C
G
Median Fluorescence Intensity (MFI)
2G12
PGT126
PGT151
3BNC117
PG9
F240
17b
A32
C11
HIVIG
bnAbs
nnAbs
D
H
**
ns

Figure 2

A

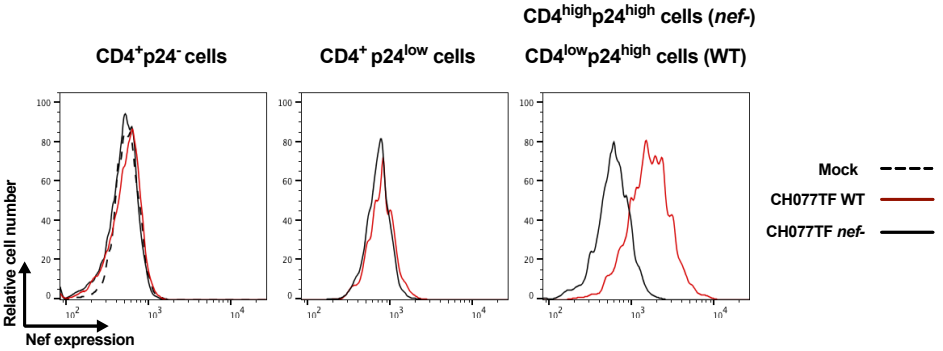
CD4+p24- cells
CD4+ p24low cells
CD4highp24high cells (nef-)
CD4lowp24high cells (WT)
Relative cell number
Nef expression
Mock
CH077TF WT
CH077TF nef-

B

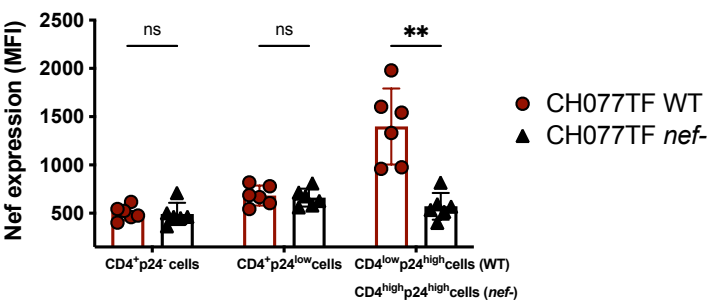
Nef expression (MFI)
ns
ns
**
CD4+p24- cells
CD4+p24lowcells
CD4lowp24highcells (WT)
CD4highp24highcells (nef-)
CH077TF WT
CH077TF nef-

Figure 3

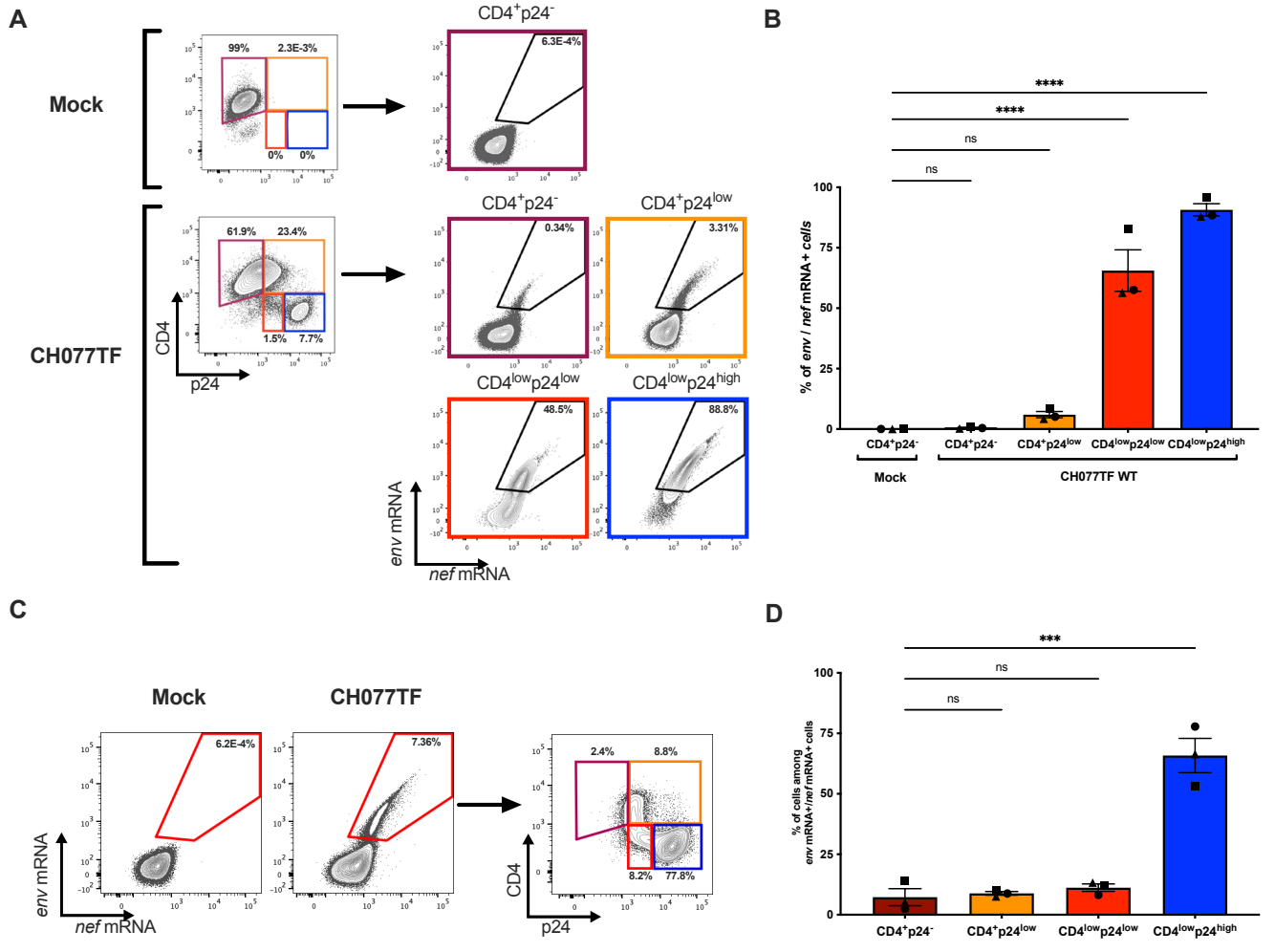
A
Mock
CH077TF
99%
2.3E-3%
0%
0%
61.9%
23.4%
1.5%
7.7%
CD4
p24
CD4+p24-
6.3E-4%
CD4+p24-
0.34%
CD4+p24low
3.31%
CD4lowp24low
48.5%
CD4lowp24high
88.8%
env mRNA
nef mRNA
B
****
****
ns
ns
% of env / nef mRNA+ cells
100
75
50
25
0
CD4+p24-
CD4+p24-
CD4+p24low
CD4lowp24low
CD4lowp24high
Mock
CH077TF WT
C
Mock
CH077TF
6.2E-4%
7.36%
env mRNA
nef mRNA
2.4%
8.8%
8.2%
77.8%
CD4
p24
D
***
ns
ns
% of cells among
env mRNA+/nef mRNA+ cells
100
75
50
25
0
CD4+p24-
CD4+p24low
CD4lowp24low
CD4lowp24high

Figure 4

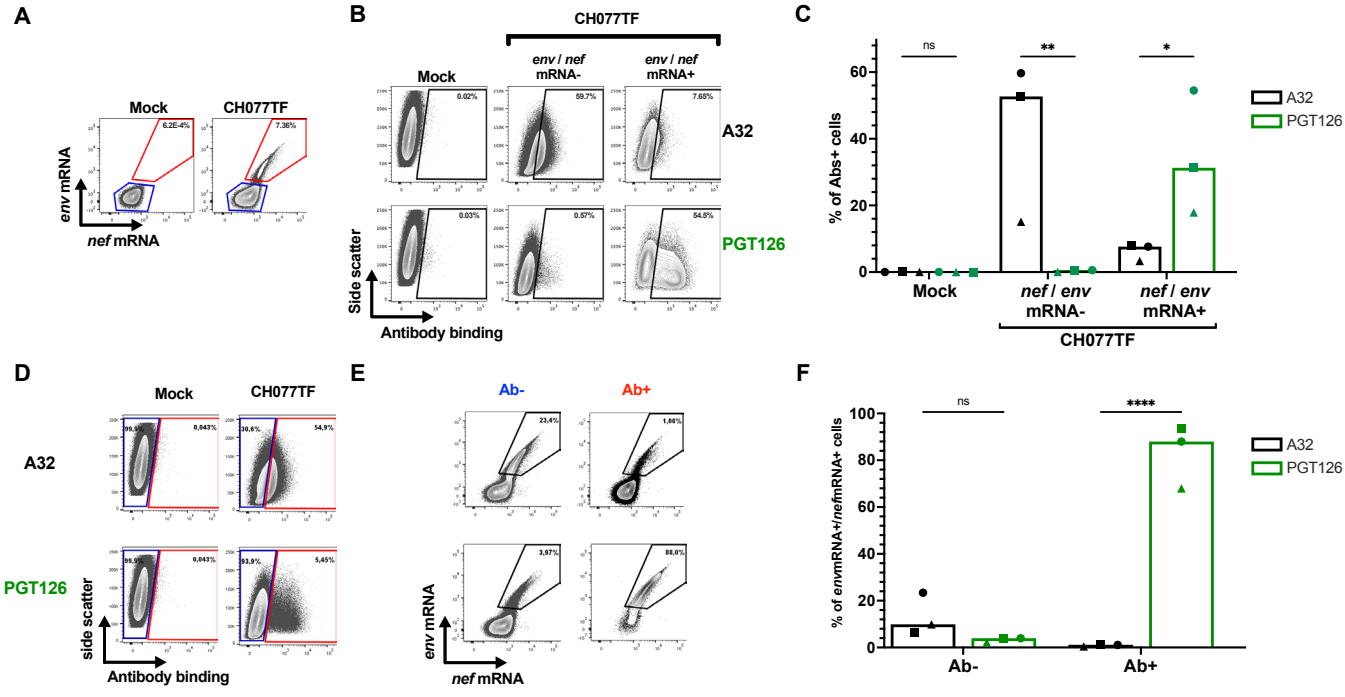
A
Mock
CH077TF
6.2E-4%
7.36%
env mRNA
nef mRNA
B
CH077TF
Mock
env / nef mRNA-
env / nef mRNA+
0.02%
59.7%
7.65%
A32
0.03%
0.57%
54.5%
PGT126
Side scatter
Antibody binding
C
ns
**
*
% of Abs+ cells
60
40
20
0
A32
PGT126
Mock
nef / env mRNA-
nef / env mRNA+
CH077TF
D
Mock
CH077TF
A32
99,9%
0,043%
30,6%
54,9%
PGT126
99,9%
0,043%
93,9%
5,45%
side scatter
Antibody binding
E
Ab-
Ab+
23,4%
1,06%
3,97%
88,0%
env mRNA
nef mRNA
F
ns
****
% of envmRNA+/nefmRNA+ cells
100
80
60
40
20
0
A32
PGT126
Ab-
Ab+

Figure 5

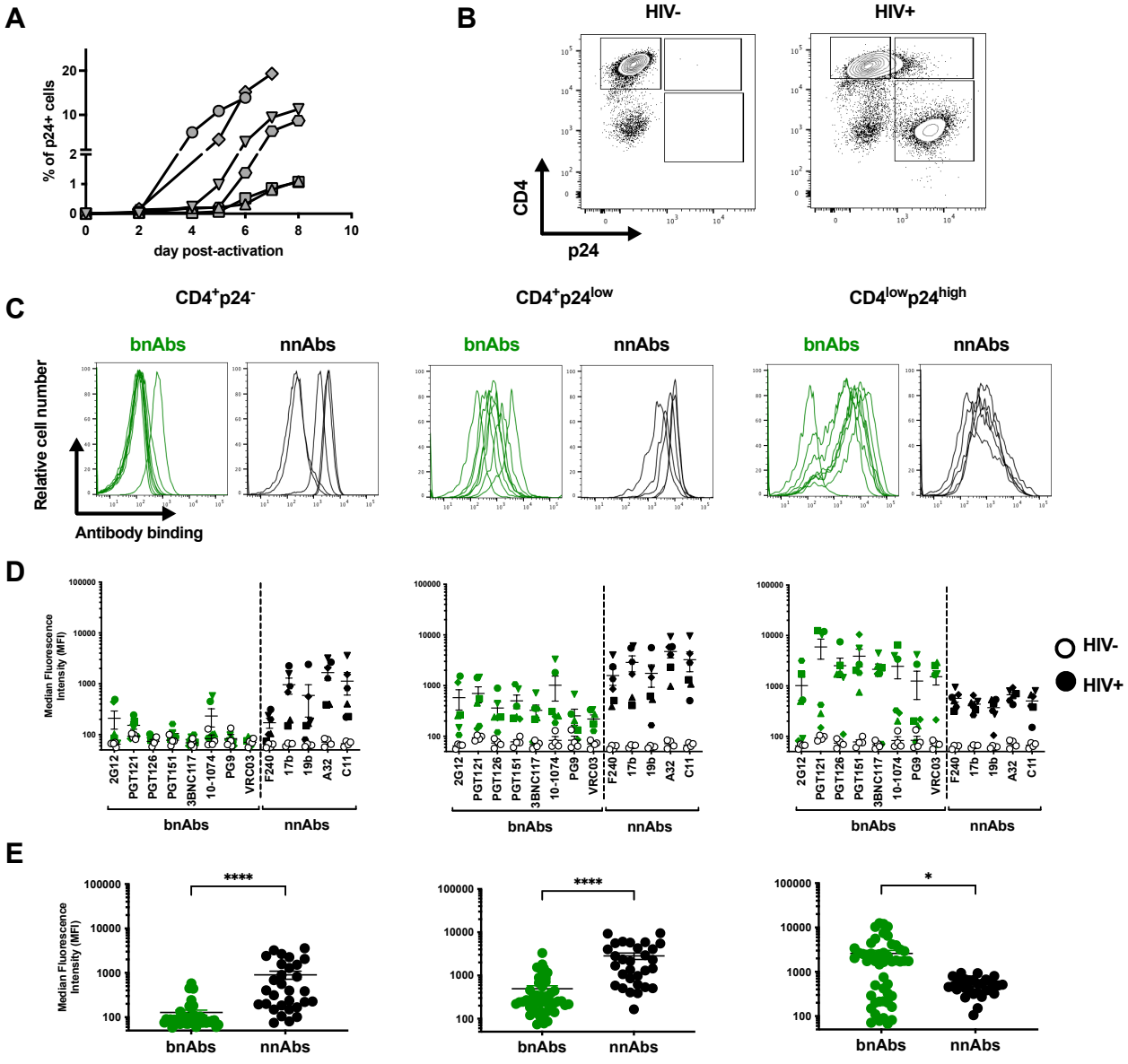
A
% of p24+ cells
day post-activation
B
HIV-
HIV+
CD4
p24
C
CD4+p24-
CD4+p24low
CD4lowp24high
bnAbs
nnAbs
Relative cell number
Antibody binding
D
Median Fluorescence Intensity (MFI)
2G12
PGT121
PGT126
PGT151
3BNC117
10-1074
PG9
VRC03
F240
17b
19b
A32
C11
bnAbs
nnAbs
HIV-
HIV+
E
Median Fluorescence Intensity (MFI)
****
*

Figure 6

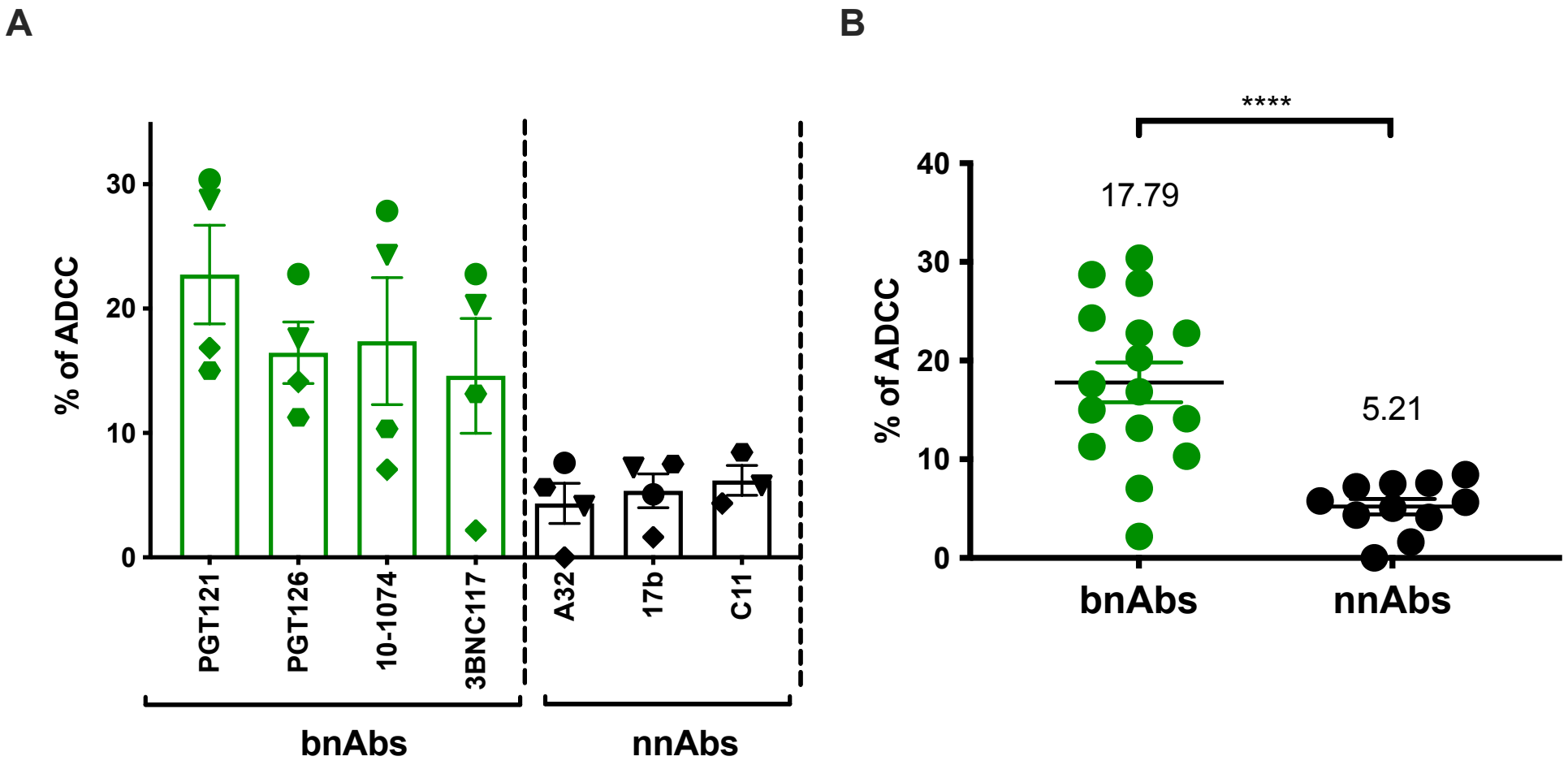
A
% of ADCC
30
20
10
0
PGT121
PGT126
10-1074
3BNC117
A32
17b
C11
bnAbs
nnAbs
B
****
% of ADCC
40
30
20
10
0
17.79
5.21
bnAbs
nnAbs

Figure 7

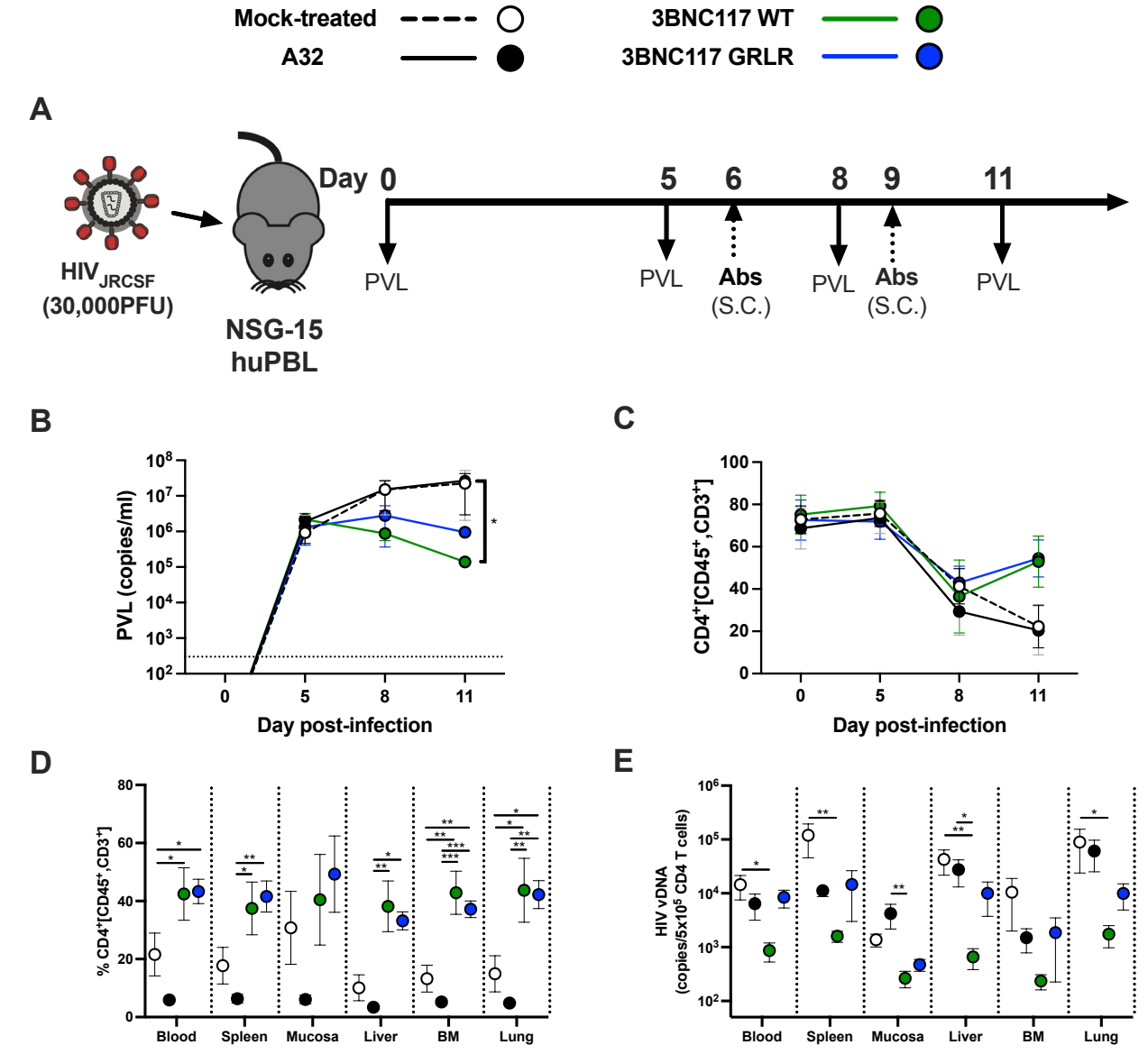
Mock-treated
A32
3BNC117 WT
3BNC117 GRLR
A
HIV JRCSF
(30,000PFU)
NSG-15
huPBL
Day 0
5
6
8
9
11
PVL
PVL
Abs
(S.C.)
PVL
Abs
(S.C.)
PVL
B
PVL (copies/ml)
Day post-infection
C
CD4+[CD45+,CD3+]
Day post-infection
D
% CD4+[CD45+,CD3+]
Blood
Spleen
Mucosa
Liver
BM
Lung
E
HIV vDNA
(copies/5x10^5 CD4 T cells)
Blood
Spleen
Mucosa
Liver
BM
Lung

SUPPLEMENTAL FIGURE LEGENDS

Figure S1. Impact of the D368R mutation on nnAbs and bnAbs binding.

Primary CD4+ T cells, mock-infected or infected with the transmitted-founder virus CH077, either expressing the wild-type (WT) or D368R Env (D368R) were stained with a panel of bnAbs and nnAbs, followed with appropriate secondary Abs. Cells were then stained for cell-surface CD4 prior detection of intracellular HIV-1 p24. (A) Graphs shown represent the median fluorescence intensities (MFI) obtained for at least 3 independent staining with the different mAbs. Error bars indicate means ± standard errors of the means. (B) Graphs shown represent the mean MFI obtained with each mAbs. (C) Percentage of the different cell populations at 48h post-infection. Statistical significance was tested using Mann-Whitney U test (** $p<0.01$, ns: non-significant).

Figure S2. Recognition of cells infected with HIV-1 constructs expressing lab-adapted and primary Envs by bnAbs and nnAbs.

Primary CD4+ T cells, mock-infected or infected with NL4.3 infectious molecular clones (IMC) expressing Env from lab-adapted (BaL, NL4.3) or primary (CH040TF, CH058, YU2, SF162) viruses were stained with a panel of bnAbs and nnAbs, followed with appropriate secondary Abs. Cells were then stained for cell-surface CD4 prior detection of intracellular HIV-1 p24. (A) Graphs shown represent the median fluorescence intensities (MFI) obtained for at least 3 independent staining with the different mAbs. Error bars indicate means ± standard errors of the means. (B) Graphs shown represent the mean MFI obtained with each mAbs for each HIV-1 IMC. (C-D) Percentage of the (C) $CD4^{low}p24^{high}$ and (D) $CD4^{+}p24^{low}$ populations at 48h post-infection. Statistical significance was tested Mann-Whitney U test (* $p<0.05$, ** $p<0.01$, **** $p<0.0001$).

Figure S3. CD4 downregulation precedes Env expression.

Primary CD4+ T cells, mock-infected or infected with the transmitted-founder virus CH077 WT were stained for cell-surface CD4 prior detection of intracellular HIV-1 p24 and *Env* mRNA and *nef* mRNA by RNA-flow FISH. (A) Example of RNA-flow FISH detection of *env* mRNA among the $CD4^{+}p24^{-}$, $CD4^{+}p24^{low}$, $CD4^{low}$ $p24^{low}$ or $CD4^{low}$ $p24^{high}$ cell populations. (C) Quantification of the percentage of *env* mRNA+ cells detected among the different cell population with three different donors. Statistical significance was tested using one way ANOVA with a Holm-Sidak post-test (* $p<0.05$, ** $p<0.01$, ns: non-significant).

Figure S4. Cells targeted by A32 are *env* mRNA negative.

Primary CD4+ T cells, mock-infected or infected with the transmitted-founder virus CH77 WT were stained with A32 or PGT126, followed with appropriate secondary Abs. Cells were then stained for cell-surface CD4 prior detection of intracellular HIV-1 p24 and *Env* mRNA and *nef* mRNA by RNA-flow FISH. (A) Histograms depicting representative *env* mRNA detection on A32+ or PGT126+ cells. (B) Median fluorescence intensities (MFI) of *env* mRNA obtained with 3 different donors. Statistical significance was tested using a Kruskal-Wallis test with a Dunn's post-test. (* $p<0.05$, ns: non-significant)

Figure S5. Nef expression in *ex vivo* expanded CD4+ T cells isolated from PLWH.

Ex vivo expanded CD4 T cells from 6 HIV+ individuals and 4 HIV- individuals were stained for surface CD4 prior to detection of intracellular Nef and p24. (A) Histograms depicting representative staining. (B) Median fluorescence intensities (MFI) obtained with 6 HIV+ individuals and 4 HIV- individuals. Statistical significance was tested using one-way ANOVA test with a Holm-Sidak post-test (**** $p<0.0001$, ns: non-significant).

Figure S6. A32 reduces the levels of CD4+ T cells in tissues *in vivo*. NSG-15-Hu-PBL mice were infected with HIV-1 JRCSF intraperitoneally. At day 6 and 9 post infection, mice were administered 1.5 mg of A32 mAb subcutaneously (s.c.). The percentage of CD4+ T cells was evaluated by flow cytometry in blood, spleen, mucosa, liver, bone marrow (BM) and lung at day 11 post-infection. Statistical significance was tested using a Mann Whitney U test (** $p<0.01$).

Figure S1

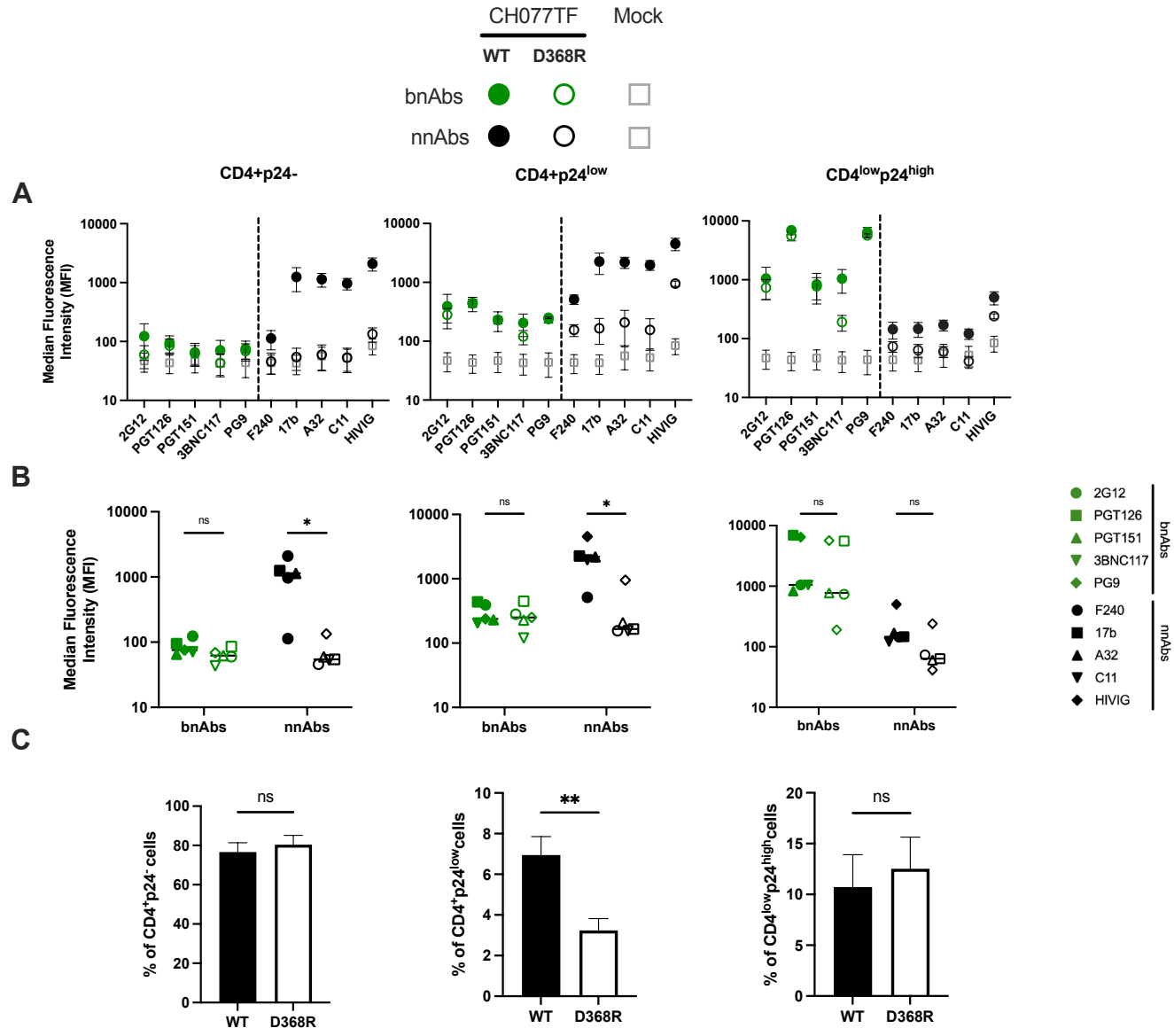
CH077TF
Mock
WT
D368R
bnAbs
nnAbs
A
CD4+p24-
CD4+p24low
CD4lowp24high
Median Fluorescence Intensity (MFI)
10000
1000
100
10
2G12
PGT126
PGT151
3BNC117
PG9
F240
17b
A32
C11
HIVIG
B
ns
*
bnAbs
nnAbs
2G12
PGT126
PGT151
3BNC117
PG9
F240
17b
A32
C11
HIVIG
C
% of CD4+p24- cells
% of CD4+p24low cells
% of CD4lowp24high cells
**
WT
D368R

Figure S2

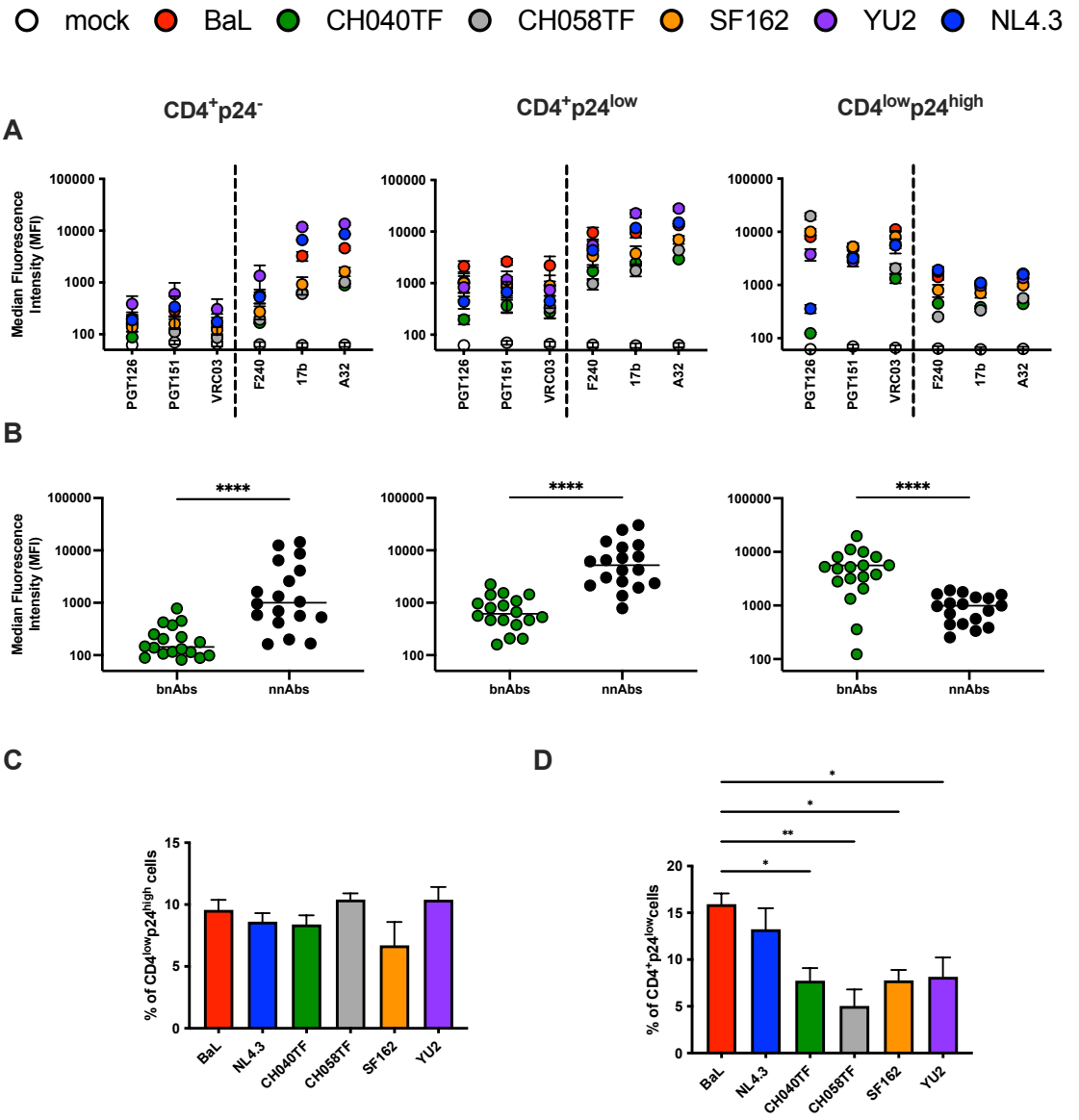
mock
BaL
CH040TF
CH058TF
SF162
YU2
NL4.3
A
CD4+p24-
CD4+p24low
CD4lowp24high
Median Fluorescence Intensity (MFI)
100000
10000
1000
100
PGT126
PGT151
VRC03
F240
17b
A32
B
****
bnAbs
nnAbs
C
% of CD4lowp24high cells
15
10
5
0
BaL
NL4.3
CH040TF
CH058TF
SF162
YU2
D
*
**
% of CD4+p24lowcells
20

Figure S3

A

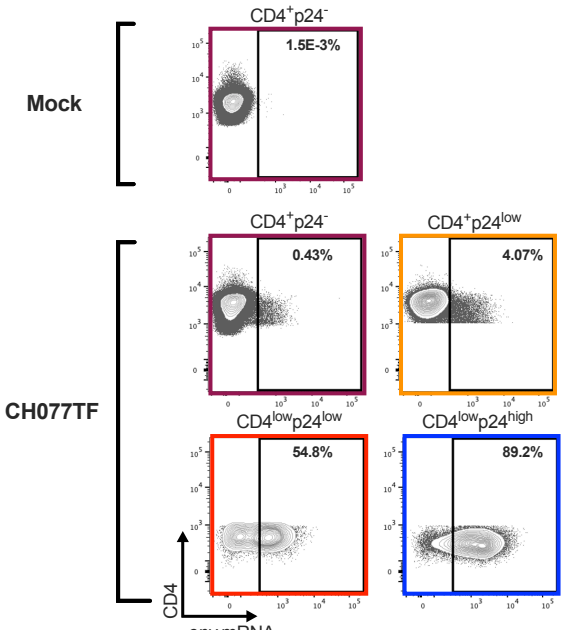
Mock
CH077TF
CD4+p24-
1.5E-3%
CD4+p24-
0.43%
CD4+p24low
4.07%
CD4lowp24low
54.8%
CD4lowp24high
89.2%
CD4
env mRNA

B

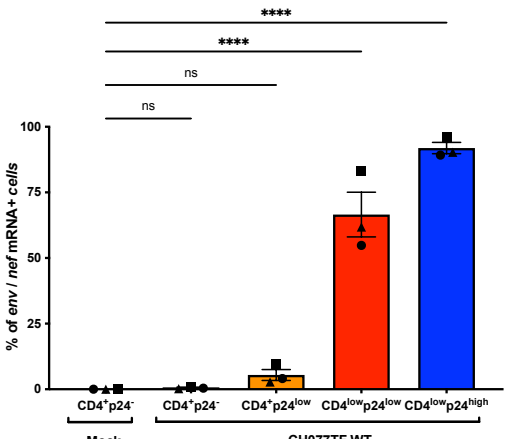
****
****
ns
ns
% of env / nef mRNA+ cells
100
75
50
25
0
CD4+p24-
CD4+p24-
CD4+p24low
CD4lowp24low
CD4lowp24high
Mock
CH077TF WT

Figure S4

A

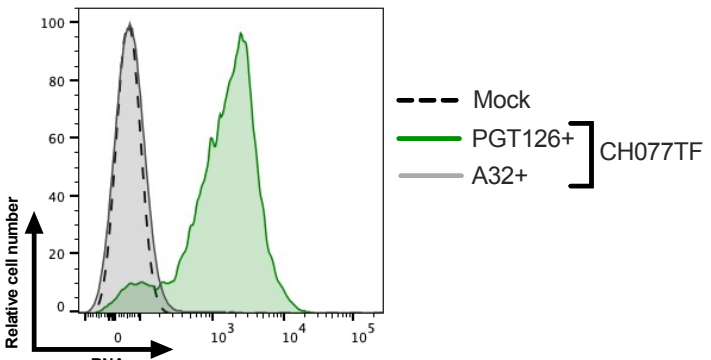
100
80
60
40
20
0
Relative cell number
0
10^3
10^4
10^5
env mRNA
Mock
PGT126+
A32+
CH077TF

B

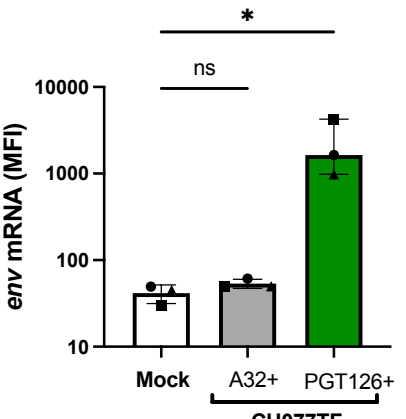
*
ns
10000
1000
100
10
env mRNA (MFI)
Mock
A32+
PGT126+
CH077TF

Figure 5

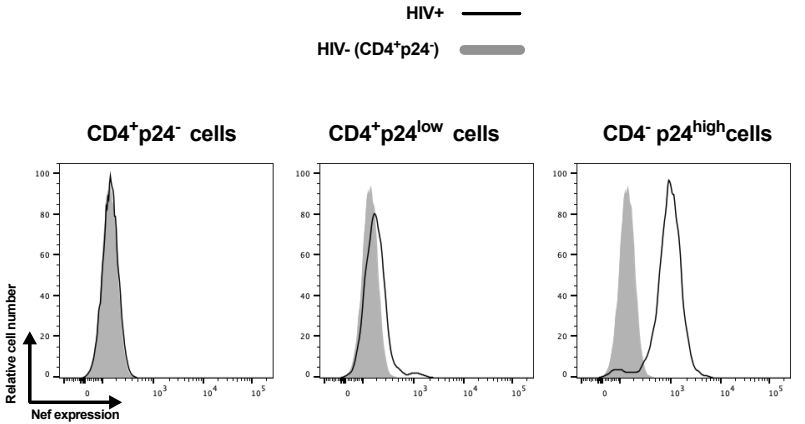
HIV+
HIV- (CD4+p24-)
A
CD4+p24- cells
CD4+p24low cells
CD4- p24high cells
Relative cell number
Nef expression

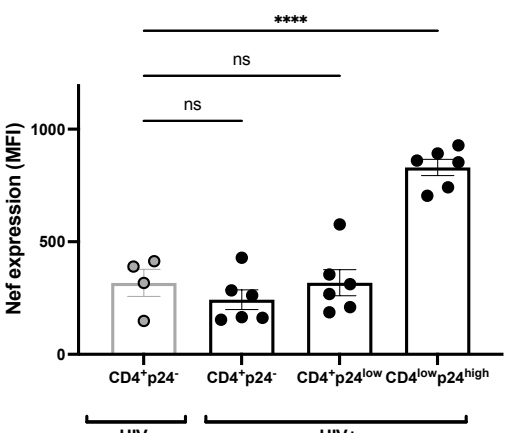
B
****
ns
ns
Nef expression (MFI)
1000
500
0
CD4+p24-
CD4+p24-
CD4+p24low
CD4lowp24high
HIV-
HIV+

Figure S6

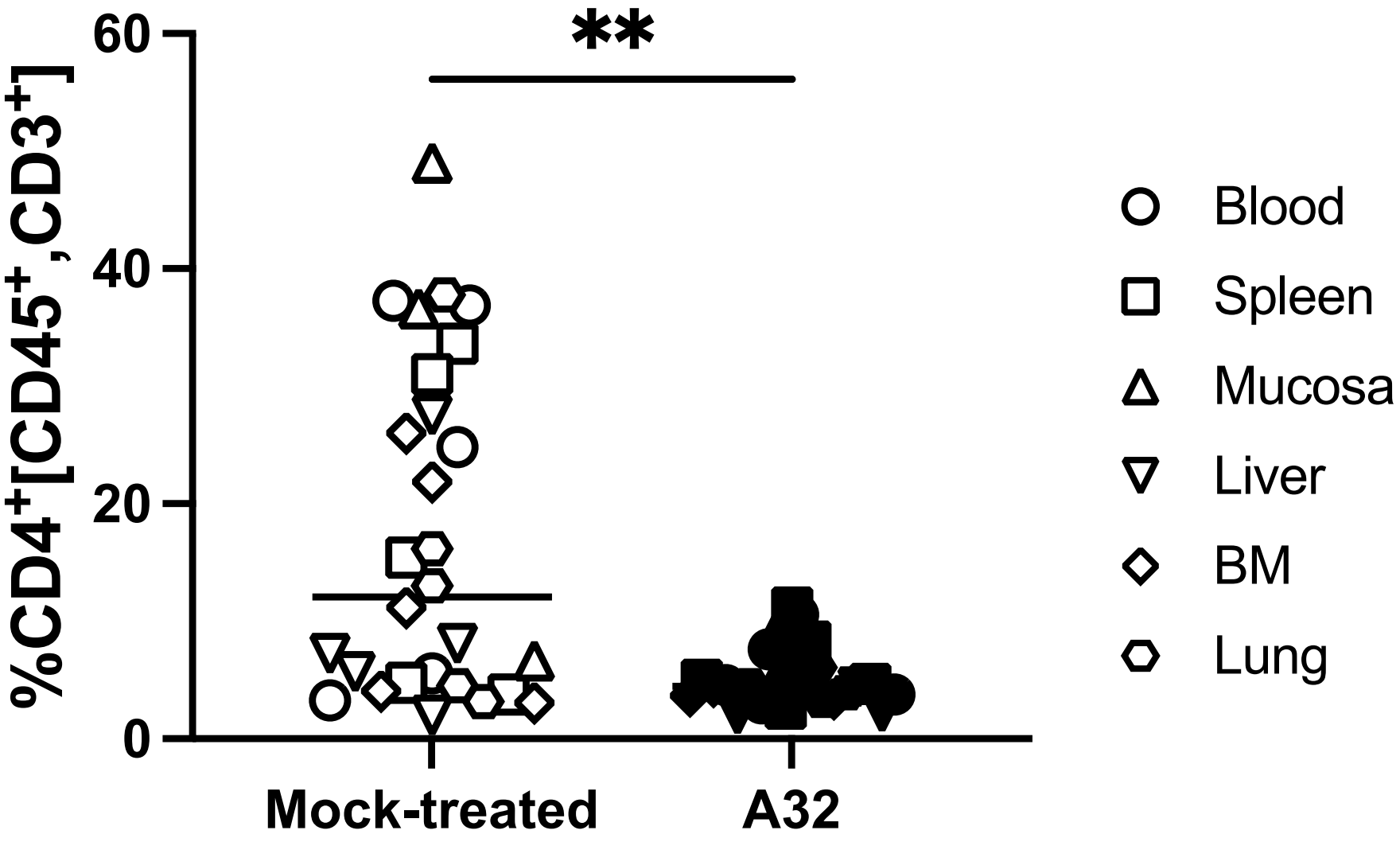
**
60
40
20
0
%CD4+[CD45+,CD3+]
Mock-treated
A32
Blood
Spleen
Mucosa
Liver
BM
Lung